MODELING THE POWER DISTRIBUTION NETWORK OF A VIRTUAL CITY AND STUDYING THE IMPACT OF FIRE ON THE ELECTRICAL INFRASTRUCTURE

A Thesis

by

ARIJIT BAGCHI

Submitted to the Office of Graduate Studies of
Texas A&M University
in partial fulfillment of the requirements for the degree of

MASTER OF SCIENCE

December 2009

Major Subject: Electrical Engineering

MODELING THE POWER DISTRIBUTION NETWORK OF A VIRTUAL CITY AND STUDYING THE IMPACT OF FIRE ON THE ELECTRICAL INFRASTRUCTURE

A Thesis

by

ARIJIT BAGCHI

Submitted to the Office of Graduate Studies of
Texas A&M University
in partial fulfillment of the requirements for the degree of

MASTER OF SCIENCE

Approved by:

Co-Chairs of Committee,	Chanan Singh
	Alexander Sprintson
Committee Members,	Garng M. Huang
	Thomas E. Wehrly
Head of Department,	Costas N. Georghiades

December 2009

Major Subject: Electrical Engineering

ABSTRACT

Modeling the Power Distribution Network of a Virtual City and Studying the Impact of Fire on the Electrical Infrastructure. (December 2009)

Arijit Bagchi, B.E., Birla Institute of Technology, MESRA, India

Co-Chairs of Advisory Committee: Dr. Chanan Singh
Dr. Alexander Sprintson

The smooth and reliable operation of key infrastructure components like water distribution systems, electric power systems, and telecommunications is essential for a nation's economic growth and overall security. Tragic events such as the Northridge earthquake and Hurricane Katrina have shown us how the occurrence of a disaster can cripple one or more such critical infrastructure components and cause widespread damage and destruction. Technological advancements made over the last few decades have resulted in these infrastructure components becoming highly complicated and inter-dependent on each other. The development of tools which can aid in understanding this complex interaction amongst the infrastructure components is thus of paramount importance for being able to manage critical resources and carry out post-emergency recovery missions.

The research work conducted as a part of this thesis aims at studying the effects of fire (a calamitous event) on the electrical distribution network of a city. The study has been carried out on a test bed comprising of a virtual city named Micropolis which was modeled using a Geographic Information System (GIS) based software package. This

report describes the designing of a separate electrical test bed using Simulink, based on the GIS layout of the power distribution network of Micropolis. It also proposes a method of quantifying the damage caused by fire to the electrical network by means of a parameter called the Load Loss Damage Index (LLDI). Finally, it presents an innovative graph theoretic approach for determining how to route power across faulted sections of the electrical network using a given set of Normally Open switches. The power is routed along a path of minimum impedance.

The proposed methodologies are then tested by running numerous simulations on the Micropolis test bed, corresponding to different fire spread scenarios. The LLDI values generated from these simulation runs are then analyzed in order to determine the most damaging scenarios and to identify infrastructure components of the city which are most crucial in containing the damage caused by fire to the electrical network. The conclusions thereby drawn can give useful insights to emergency response personnel when they deal with real-life disasters.

ACKNOWLEDGMENTS

I would like to thank my advisor, Dr. Chanan Singh, for the extensive support and guidance he provided me throughout the course of this research work. I would also like to thank my co-advisor, Dr. Alexander Sprintson, for his constant encouragement towards the successful completion of my thesis.

Special thanks to my other committee members as well – Dr. Garng M. Huang and Dr. Thomas E. Wehrly – for all their time and support. Thank you Dr. Wehrly for agreeing to join my committee at such short notice.

Thanks are also due to Ian Horbaczewski and Kimberley Jones for their contributions to the modeling of the electrical distribution network of Micropolis using ArcMap, to Jacob Torres for all the help and guidance he provided me regarding working with ArcMap, to Dr. Elizabeth C. Bristow for her help with the MUFS code and MUFS files, to Susan Louis for her help with formatting this document and finally, to my family and friends for their continuous support and encouragement.

This work was supported in part by NSF Grant EECS – 0725823.

TABLE OF CONTENTS

CHAPTER Page

LIST OF FIGURES

LIST OF TABLES

CHAPTER I

INTRODUCTION

The U.S.A. PATRIOT Act of 2001 [1] defines the term "Critical Infrastructure" as "systems and assets, whether physical or virtual, so vital to the United States that the incapacity or destruction of such systems and assets would have a debilitating impact on security, national economic security, national public health or safety or any combination of those matters." The Critical Infrastructure Protection (CIP) Program [2], as set forth through the Presidential Decision Directive (PDD - 63) of May 1998, identifies the following sectors as key to the smooth functioning of any modern day society: telecommunications, energy, water systems and emergency services, transportation and banking and finance. With the advent of cutting-edge technologies leading to ever increasing levels of automation in our daily lives, these infrastructure components have not only become increasingly complicated but also heavily inter-dependent on each other. The development of models ([3] – [6]) which can simulate this complex interaction amongst the infrastructure components is thus an important area of research, as they might be helpful for civic authorities and emergency response personnel when they deal with an actual disaster.

The research work conducted as a part of this thesis proposes a methodology to study and quantify the damage caused by fire to the electrical distribution network of a

---

This thesis follows the style of *IEEE Transactions on Power Delivery*.

city. The fire is assumed to be initiated either by natural means, e.g. a lightning stroke or a wildfire; or deliberately, e.g. a terrorist attack. This study has been carried out on a test bed comprising of a virtual city named Micropolis, which was laid out using a Geographic Information System (GIS) based software package by researchers at the Department of Civil Engineering and the Department of Electrical and Computer Engineering here at Texas A&M University. The remainder of this report has been structured in the following fashion.

Chapter II gives an overview of the layout of the virtual city of Micropolis [7] along with its civil and electrical ([8] – [9]) infrastructure components.

Chapter III briefly describes the Model of Urban Fire Spread (MUFS) [10], which is a software package used to simulate an urban fire along with its subsequent suppression.

Chapter IV describes the modeling of a separate electrical test bed using Simulink, based on the GIS layout of the power distribution network of Micropolis. It discusses the methodology used for determining the distribution transformer ratings ([11] – [12]), lists the standard formulae used for calculating the line parameters (impedance and capacitance values per unit length) ([13] – [16]) and describes the operation of the protection system components (relays, isolators and breakers) ([17] – [18]) of the distribution network of Micropolis.

Chapter V proposes a methodology for studying the effects of fire on the electrical distribution network of a city. It lists the relevant assumptions, definitions and algorithms [8] pertaining to the development and the implementation of the proposed

methodology. The damage caused by fire to the electrical infrastructure is then quantified by means of the Load Loss Damage Index (LLDI) [8], also presented in this chapter.

Chapter VI describes the various conclusions drawn from running numerous simulations on the Micropolis test bed corresponding to different fire spread scenarios, and comparing the LLDI values thereby generated.

Chapter VII proposes a graph theoretic approach for determining how to route power across faulted sections of the distribution network using a given set of Normally Open (NO) switches. The power routing is done through a path of minimum impedance so as to reduce the voltage drop at the farthest end.

Chapter VIII incorporates the power routing methodology proposed in Chapter VII into the simulations run as a part of Chapter VI, and presents the important conclusions drawn from the comparison and analysis of the generated LLDI values.

Chapter IX summarizes this research work by presenting the general conclusions.

CHAPTER II

LAYOUT OF VIRTUAL CITY MICROPOLIS

The September 11, 2001 terrorist attacks on the World Trade Center prompted the United States government to start treating all information related to a city's infrastructure layout as classified. While on one hand this prevents the misuse of such information by malicious elements, it also makes it difficult for researchers to test their developed models with real life data. The designing of a virtual city with all the key infrastructure components embedded in it is thus an important part of any research work conducted in this area.

The virtual city of Micropolis, as represented by the layout of Fig. 2.1, was designed for the purpose of it being used as a test bed for carrying out studies on the effects of disasters on the interdependent infrastructure components of a city. Micropolis was developed using GIS (ArcMap) and hydraulic modeling (EPANet) based software, as described in [7]. The electrical distribution network of the city was then modeled and its corresponding components added to the GIS layout of [7], as described in [8]. Micropolis, a city of around 5000 residents, covers an area of approximately 2 square miles. To make the design as realistic as possible, a developmental timeline of 130 years was taken into consideration [7]. While this timeline is manifested by the choice of pipe material, pipe diameter etc. for the civil infrastructure model, it does not have a significant impact on the electrical modeling as most electrical components are either upgraded or replaced after every 30-40 years [9].

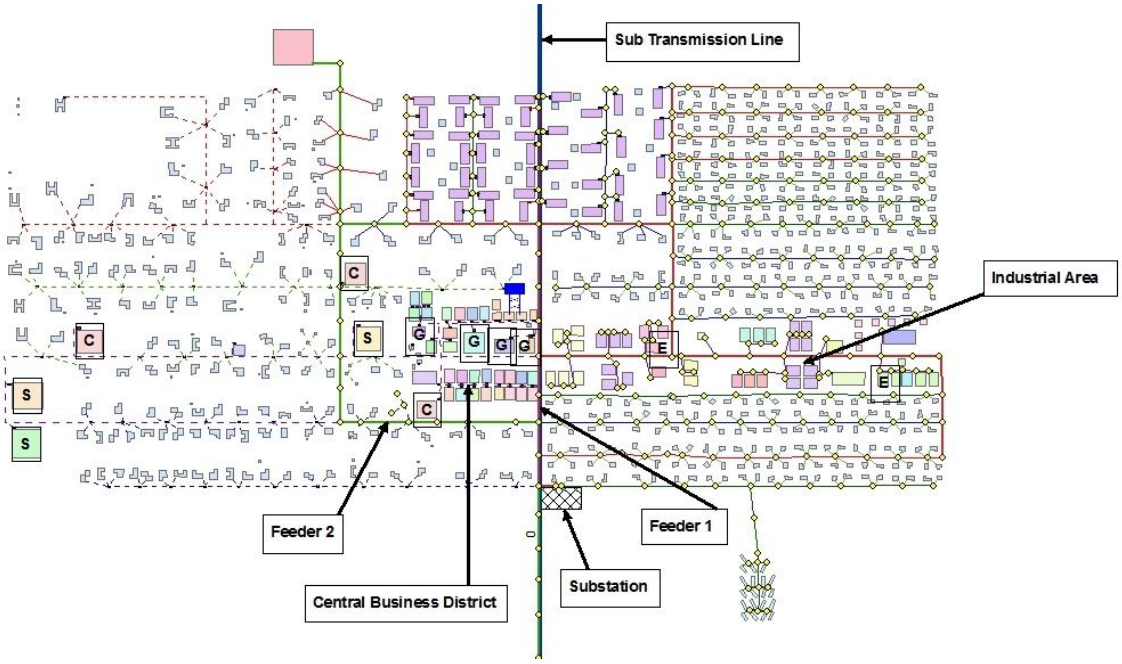

Fig. 2.1. Layout of the electrical infrastructure components for the city of Micropolis.

It is assumed that Micropolis does not have a power generation facility of its own, but it obtains its power from a sub-transmission line (138 KV rating) running through the heart of the city, as shown in Fig. 2.1. The city has just one substation, where the sub-transmission level voltage of 138 KV is stepped down to the distribution level voltage of 13.8 KV [8]. Two three-phase feeder lines (each of 13.8 KV rating) emanate from the substation, and by repeated branching off into smaller three-phase sub-branches and finally into single-phase laterals, they deliver the power from the substation across the entire city. Overhead conductors are represented by the solid lines of Fig. 2.1; while underground cables are shown using dotted lines. The overhead conductors are supported on wooden poles, which are represented by the yellow dots in Fig. 2.1. Distribution transformers rated 100 KVA or above are pad-mounted, while

others are mounted on the poles unless they are fed by underground cables (in which case they are always pad-mounted) ([8] – [9]). All pad-mounted distribution transformers are assumed to be enclosed in iron casings.

For simplicity sake, the customer end supply voltages and the amount of load consumed by users across Micropolis have been categorized into few distinct profiles, as shown in Table 2.1 [8]. Finally, important information about loading of individual feeders and of the total system is as shown in Table 2.2 ([8] – [9]).

TABLE 2.1
VOLTAGE AND LOAD PROFILES FOR CONSUMERS ACROSS MICROPOLIS

Voltage Profiles	
Customer Type	**Voltage Ratings**
Residential (Feeders 1 & 2)	120 V, 1-Φ
City Churches and Schools	208 V, 3-Φ
Industrial (Feeder 1)	208 V, 3-Φ or 3.3 KV, 3-Φ
Central Business District (Feeder 2)	208 V, 3-Φ
Load Profiles	
Customer Type	**Load Consumed**
Residential (Feeder 1)	5 KVA
Residential (Feeder 2)	7 KVA
City Churches	250 KVA
City Schools	300 KVA
Industrial (Feeder 1)	30/75/150/225 KVA
Central Business District (Feeder 2)	30/45/150/250 KVA

TABLE 2.2
SYSTEM AND INDIVIDUAL FEEDER LOADING INFORMATION

	Residential	**Commercial/Industrial**	**Total**
Feeder 1	6840 KVA	3180 KVA	10020 KVA
Feeder 2	1183 KVA	3922.5 KVA	5105.5 KVA
System	8023 KVA	7102.5 KVA	15125.5 KVA

CHAPTER III

MODEL OF URBAN FIRE SPREAD (MUFS)

The Model of Urban Fire Spread (MUFS), as described and tested in [10], is a numerical tool used to simulate an urban fire starting from one or more user-defined points of ignition. The model calculates the extent of the fire spread area, taking into consideration the fire suppression efforts made by the community's emergency response personnel. To determine the efficiency of fire suppression, MUFS also takes into account the simultaneous (i.e., along with the spread of fire) damage or destruction of one or more supporting infrastructures for fire response (e.g., water distribution system, telecommunication networks, etc.) [10]. The following sections briefly describe the various inputs and outputs pertaining to a given fire spread simulation run using MUFS.

3.1. MUFS Simulation Input Parameters

The MUFS code requires the following user-defined inputs in order to run a given fire spread simulation.

3.1.1. Supporting Infrastructure Damage Profile (SIDP)

For the purpose of this thesis, ten different damage profiles corresponding to one or more supporting infrastructures for fire response have been considered, as shown in Table 3.1 [8].

3.1.2. Urban Fire Ignition Points (UFIP)

The extent of fire spread damage will not only depend on the particular SIDP selected, but also on the specific point(s) of ignition of fire chosen for a given simulation

[10]. For the purpose of this thesis, four different fire ignition point profiles have been considered, as shown in Table 3.2 [8].

3.1.3. Wind Direction

As the rate of spread of fire will be the highest along the direction of flow of wind, varying the wind direction for a given SIDP and UFIP combination will give rise to a quite different fire spread scenario [10]. For the purpose of this research, four cardinal wind directions have been considered: East, West, North and South [8].

TABLE 3.1
SUPPORTING INFRASTRUCTURE DAMAGE PROFILE (SIDP)

Damage Profile	Remarks
A01	All three high-service pumps of Micropolis permanently taken out of service.
A03	One out of the three high-service pumps of Micropolis permanently taken out of service.
B03	All three high-service pumps of Micropolis temporarily taken out of service after two hours since start of simulation, for a duration of two hours.
D01	Elevated storage tank of Micropolis unavailable for the entire duration of the simulation.
D02	Elevated storage tank of Micropolis becomes unavailable after an hour since start of simulation, and remains so till simulation ends.
AD1	Combination of profiles A01 and D02.
E02	Water main breach near the Central Business District.
F01	Water contamination (and subsequent isolation) at south-east side of town.
F04	Water contamination (and subsequent isolation) in highest-density residential area towards north-east side of town.
UND	No supporting infrastructures damaged. This profile has been deliberately included in order to compare its effects vis-à-vis those of the others.

TABLE 3.2
URBAN FIRE IGNITION POINTS (UFIP)

Ignition Point Acronym	Remarks
GOV	Government Buildings (Community Center, City Hall, Post Office and Rail Museum), represented by buildings marked ‘G’ in Fig. 2.1.
SCH	City Schools, represented by buildings marked ‘S’ in Fig. 2.1.
CHU	City Churches, represented by buildings marked ‘C’ in Fig. 2.1.
ECO	Ecological targets (Printing Press and Timber Mill), represented by buildings marked ‘E’ in Fig. 2.1.

By considering different combinations of such SIDPs, UFIP profiles and wind directions; a variety of ‘fire spread scenarios’ can therefore be generated.

3.2. MUFS Simulation Outputs

Once all relevant user-defined inputs have been provided to MUFS, it is ready to run the concerned fire spread simulation. A constant wind speed of 10 mph is assumed for all simulation runs. A particular simulation run corresponds to 12 hours of physical fire spread. Starting from a user-defined point of ignition, the model calculates the incremental distance advanced by the fire every five minutes. It is assumed that the fire spreads along the direction of each of the four ‘fire spread vectors’, the orientations of which are determined with respect to the dominant wind direction as: ‘downwind’ (along the flow of wind), ‘upwind’ (opposite to wind flow), ‘sidewind right’ (90° to the right of ‘downwind’) and ‘sidewind left’ (opposite to ‘sidewind right’) [10]. The ‘fire polygon’ thus created by joining the tips of the fire spread vectors for a given time step is therefore a quadrilateral, and it represents the area covered by the fire until that time. The MUFS program thus essentially outputs the fire polygon vertex coordinates after every five minutes until the end of simulation (corresponding to 12 hours of physical fire spread).

CHAPTER IV

DESIGNING OF ELECTRICAL TEST BED USING SIMULINK

This chapter describes the designing of an electrical test bed, which has been modeled using Simulink (MATLAB) based on the GIS layout of the electrical distribution network of Micropolis [8]. Fig. 4.1 presents a snapshot of the layout of the electrical infrastructure components as modeled in the test bed. The following sections explain the different stages in the design phase in a step-by-step fashion.

4.1. Determination of Distribution Transformer Constants

Fig. 4.2A shows the equivalent circuit of a transformer, with all secondary parameters (impedance, current, voltage) referred to the primary. The turns ratio of the transformer is denoted by 'a'. Since the magnetizing current I_o is only a small fraction of the full load primary current, $I_2^{'}$ in Fig. 4.2A is practically equal to I_1 [11]. Therefore, the equivalent circuit of Fig. 4.2A can be further approximated into the circuit of Fig. 4.2B.

Transformer constants are usually calculated by performing open circuit and short circuit tests on a given machine. Since such test data is not easily available for all the different transformer configurations used across the electrical network of Micropolis, we use the '%Z' and 'X/R' values available in standard tables [12] for our calculations.

4.1.1. Determination of Magnetizing Branch Constants

Assuming the base voltage 'V_b' and the base power 'S_b' for the circuit of Fig. 4.2B to be equal to the nominal voltage of winding 1 'V_1' and the nominal power rating of the transformer 'S_1' respectively, the base current 'I_b' and the base impedance 'Z_b' are

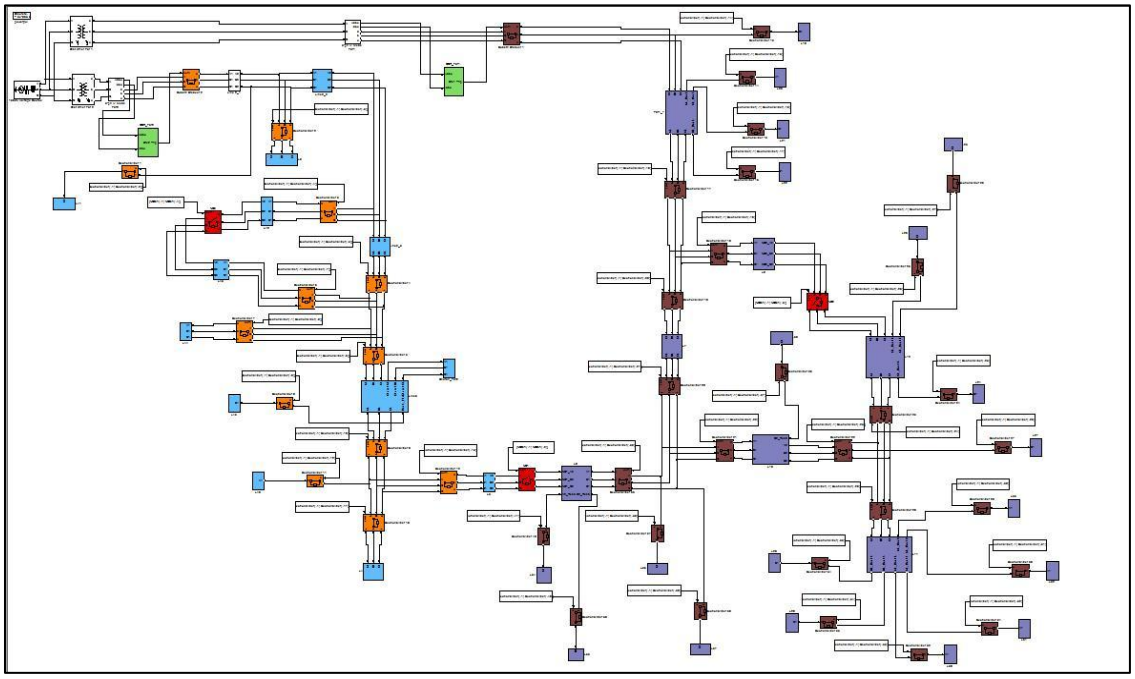

Fig. 4.1. Snapshot of the electrical test bed representing the distribution network of Micropolis.

calculated as:

$$I_b = S_b/V_b = S_1/V_1 = I_1, \text{ and } Z_b = V_b^2/S_b \quad (4.1)$$

Now, assuming that the magnetizing current I_o = 0.5% of the full load primary (winding 1) current I_1, the magnitude of the magnetizing branch impedance '$\mathbf{Z_M}$'[a] for the circuit of Fig. 4.2B is calculated as:

$$|\mathbf{Z_M}| = V_1/I_o = V_b/(0.005*I_1) = V_b/(0.005*I_b) = 200*Z_b \quad (4.2)$$

Finally, expressing $|\mathbf{Z_M}|$ in per unit yields:

$$|\mathbf{Z_M}|_{p.u} = (200*Z_b)/Z_b = 200 \text{ p.u.} \quad (4.3)$$

Assuming that the resistance and the reactance components of the magnetizing branch have equal magnitudes, we get, after some calculations, $R_o = X_o = 200\sqrt{2}$ p.u.

[a] Expressions in bold represent phasors.

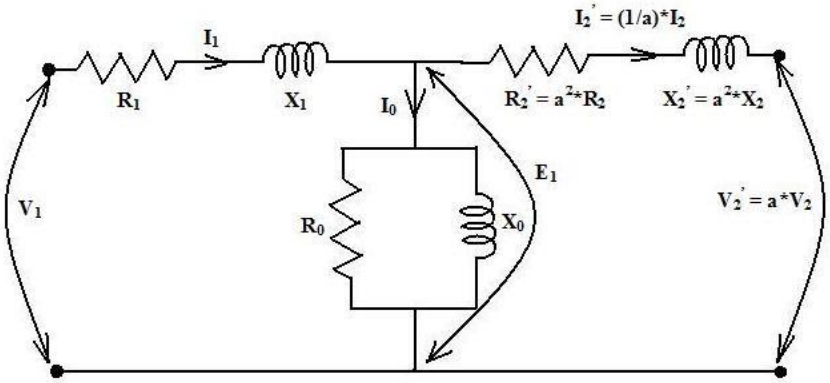

Fig. 4.2A. Equivalent circuit of a transformer.

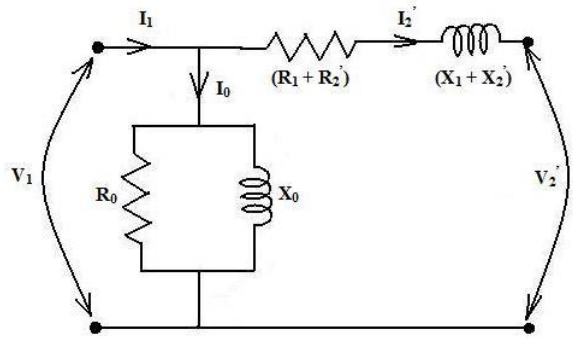

Fig. 4.2B. Approximate equivalent circuit of the transformer.

4.1.2. Determination of Primary and Secondary Winding Leakage Impedances

Using the '%Z' and the 'X/R' values available in standard tables [12], the primary and secondary winding leakage impedances are calculated in the following fashion. Assuming the '%Z' value for a given transformer is equal to 'z' p.u and its 'X/R' ratio is equal to 'b', the per unit resistance and reactance values are calculated as:

$$z/100 = \sqrt{(R_{p.u}^2 + X_{p.u}^2)} = \sqrt{(R_{p.u}^2 + b^2 * R_{p.u}^2)} = R_{p.u}\sqrt{(1 + b^2)} \quad (4.4)$$

$$R_{p.u} = z/(100*\sqrt{1 + b^2}), \text{ and } X_{p.u} = b*R_{p.u} \quad (4.5)$$

The per unit resistance and reactance values calculated using equations (4.4) and (4.5) represent the total resistance ($R_1 + R_2'$) and reactance ($X_1 + X_2'$) terms respectively,

as shown in Fig. 4.2B. It is however generally assumed that the primary and the secondary (as referred to the primary) winding leakage impedances have equal contributions to the total leakage impedance associated with the circuit of Fig. 4.2B [11]. The primary and secondary (as referred to the primary) winding leakage impedances are therefore calculated by dividing the results obtained from equation (4.5) by two. Since the resistance and reactance values calculated are already expressed in per unit, the secondary winding leakage impedance (as referred to the primary) still remains the same on being referred back to the secondary side.

4.2. Determination of Conductor Sizing Based on Ampacity

Since the load consumed by users across Micropolis have been categorized into few distinct profiles as shown in Table 2.1, the total load demand associated with a given line 'i' in the system can be calculated by adding up the individual loads associated with each downstream customer. Denoting the load demand associated with the line 'i' as 'KVA_i' and assuming 5% losses associated with the flow of power, the total power carried by the line is then given as (KVA_i/0.95). The r.m.s value of the line current is then calculated in the following fashion.

4.2.1. Single Phase Calculations

$$\mathbf{S} = \mathbf{V}.\mathbf{I}^{*},\ \mathbf{V} = V_{rms}.e^{j.\theta v},\ \text{and}\ \mathbf{I} = I_{rms}.e^{j.\theta i} \tag{4.6}$$

$$|\mathbf{S}| = |\mathbf{V}.\mathbf{I}^{*}| = |\mathbf{V}|.|\mathbf{I}^{*}| = V_{rms}.I_{rms} \tag{4.7}$$

In equations (4.6) and (4.7), the terms '**S**', '**V**' and '**I**' represent the phasors of the complex single phase power, the line-to-neutral voltage and the line current respectively. Since the distribution feeders of Micropolis are rated at 13.8 KV, the

corresponding single phase line-to-neutral voltage (r.m.s value) can be found to be equal to 13.8/√3, or, 8 KV (assuming balanced three phase configuration of the system). The r.m.s value of the line current can thus be calculated by substituting the terms |**S**| and V_{rms} in equation (4.7) by (KVA_i/0.95) and 8 KV respectively.

4.2.2. Three Phase Calculations

$$\mathbf{S} = \mathbf{V_{an}}.\mathbf{I_{an}}^{*} + \mathbf{V_{bn}}.\mathbf{I_{bn}}^{*} + \mathbf{V_{cn}}.\mathbf{I_{cn}}^{*} \tag{4.8}$$

$$\mathbf{V_{an}} = V_{rms}.e^{j.0},\ \mathbf{V_{bn}} = V_{rms}.e^{j.(2\Pi/3)},\ \text{and}\ \mathbf{V_{cn}} = V_{rms}.e^{-j.(2\Pi/3)} \tag{4.9}$$

$$\mathbf{I_{an}} = I_{rms}.e^{-j.\Phi},\ \mathbf{I_{bn}} = I_{rms}.e^{j.(2\Pi/3\ -\ \Phi)},\ \text{and}\ \mathbf{I_{cn}} = I_{rms}.e^{-j.(2\Pi/3\ +\ \Phi)} \tag{4.10}$$

In equations (4.8) – (4.10), the term '**S**' denotes the phasor of the total three phase complex power; '$\mathbf{V_{an}}$', '$\mathbf{V_{bn}}$' and '$\mathbf{V_{cn}}$' denote the phasors of the three line-to-neutral voltages; and '$\mathbf{I_{an}}$', '$\mathbf{I_{bn}}$' and '$\mathbf{I_{cn}}$' denote the phasors of the three line currents. 'V_{rms}' and 'I_{rms}' represent the r.m.s values of the line-to-neutral voltage and the line current respectively, and 'Φ' signifies the phase difference between the voltage and the current phasors. Using equations (4.8) – (4.10) and assuming balanced three phase configuration of the system, the total three phase complex power is then given as:

$$\mathbf{S} = 3*V_{rms}*I_{rms}*e^{j.\Phi} = \sqrt{3}*V_{rms,L\text{-}L}*I_{rms}*e^{j.\Phi} \tag{4.11}$$

$$|\mathbf{S}| = \sqrt{3}*V_{rms,L\text{-}L}*I_{rms} \tag{4.12}$$

In equation (4.11), the term '$V_{rms,L\text{-}L}$' represents the r.m.s value of the three phase line-to-line voltage. Since the distribution feeders of Micropolis are rated at 13.8 KV, the r.m.s value of the line current can thus be calculated by substituting the terms |**S**| and $V_{rms,L\text{-}L}$ in equation (4.12) by (KVA_i/0.95) and 13.8 KV respectively.

Once the r.m.s values of the line currents are calculated using equations (4.7) or (4.12), they are compared with the different conductor ampacity ratings available in manufacturer specification sheets ([19] – [20]). While All Aluminum Conductor (AAC) is used for the construction of the overhead lines, the underground lines are laid using Aluminum Conductor TRXLPE Insulation Concentric Neutral cables. An appropriate ampacity rating greater than the magnitude of the line current calculated is chosen, and the corresponding conductor size is then assigned to the concerned line. Table 4.1 shows the various conductor sizings used in the modeling of the electrical test bed for Micropolis ([19] – [20]).

TABLE 4.1
MICROPOLIS ELECTRICAL TEST BED CONDUCTOR SIZINGS

Overhead Lines	
Conductor Size	**Ampacity (Amps)**
6 AWG[b]	110 A
2 AWG	195 A
3/0 AWG	350 A
4/0 AWG	410 A
266.8 kcmil[c]	475 A
397.5 kcmil	615 A
Underground Cables	
Conductor Size	**Ampacity (Amps)**
2 AWG	130 A

[b]AWG = American Wire Gage, [c]1 kcmil = 1000 circular mills = 0.5067 mm^2.

4.3. Determination of Line Parameters

Once the conductor sizings for the different overhead lines and underground cables of the electrical distribution network of Micropolis are decided, the next step is to calculate the impedance and capacitance values associated with each such line or cable. The following subsections explain the different formulae used for this purpose.

4.3.1. Underground Cables, Three Phase

The three phase underground cables present in the electrical distribution network of Micropolis consist of seven strands of 2 AWG thick Al conductors, a 175 mils thick TRXLPE insulation layer, a "one-third" concentric neutral comprising of six strands of 14 AWG thick Cu wires and a LLDPE encapsulating jacket. The cable burial configuration is as shown in Fig. 4.3. The positive (Z_1) and zero (Z_0) sequence impedances for three phase concentric neutral underground cables are calculated using the following formulae [13].

$$Z_1 = Z_{aa} - Z_{ab} - ((Z_{ax} - Z_{ab})^2/(Z_{xx} - Z_{ab})) \quad (4.13)$$

$$Z_0 = Z_{aa} + (2*Z_{ab}) - ((Z_{ax} + 2*Z_{ab})^2/(Z_{xx} + 2*Z_{ab})) \quad (4.14)$$

$$Z_{aa} = R_\Phi + R_e + j*k_1*\log_{10}(D_e/GMR_\Phi) \quad (4.15)$$

$$Z_{ab} = R_e + j*k_1*\log_{10}(D_e/GMD_\Phi) \quad (4.16)$$

$$Z_{xx} = R_N + R_e + j*k_1*\log_{10}(D_e/GMR_N) \quad (4.17)$$

$$Z_{ax} = R_e + j*k_1*\log_{10}(D_e/DN_2) \quad (4.18)$$

In equations (4.13) – (4.18), 'Z_{aa}' represents the self impedance of each phase conductor, 'Z_{ab}' represents the mutual impedance between two conductors, 'Z_{ax}' represents the mutual impedance between a phase conductor and its concentric neutral, and 'Z_{xx}' denotes the self impedance of each concentric neutral. 'R_Φ' is the resistance of each phase conductor expressed in ohms/1000 feet (data available in standard tables, [13]), 'R_N' is the resistance of the neutral (resistance of a 'one-third' neutral is thrice that of the phase conductor [13]) expressed in ohms/1000 feet, 'k_1' is equal to 0.0529 ohms/1000 feet, 'GMR_Φ' is the geometric mean radius of the phase conductor expressed

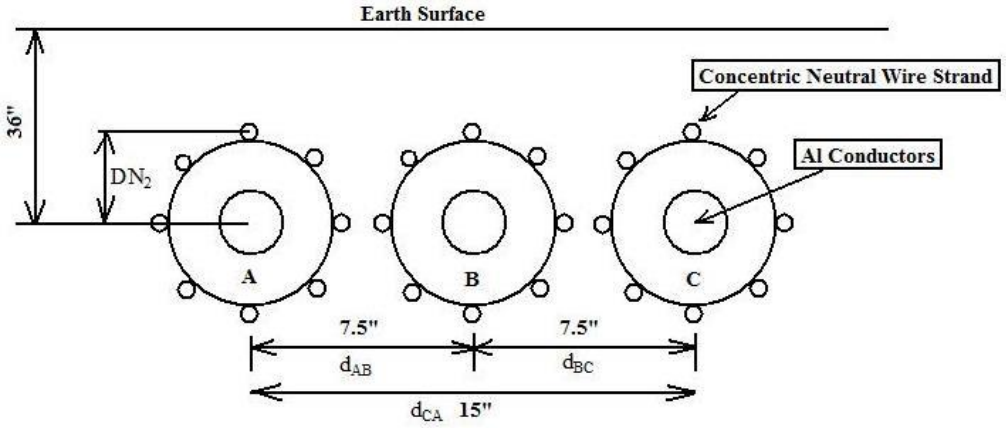

Fig. 4.3. Underground cable burial configuration.

in inches (data available in standard tables, [13]), 'GMD_{Φ}' is equal to $\sqrt[3]{d_{AB} * d_{BC} * d_{CA}}$ (inches, see Fig. 4.3.), 'R_e' is the resistance of the earth return path and is equal to 0.01807 ohms/1000 feet, 'D_e' is the equivalent depth of the earth return current and is equal to $25920\sqrt{\rho/60}$ inches, 'ρ' is the earth resistivity and is equal to 100 Ω-m, 'GMR_N' is the geometric mean radius of the concentric neutral and is equal to $\sqrt[n]{0.7788 * n * DN_2^{(n-1)} * r_n}$ inches, 'n' is the number of neutral wire strands, 'r_n' is the radius of each neutral strand in inches, and 'DN_2' is the distance from the center of the phase conductor to the center of the neutral strand (inches, see Fig. 4.3.). The sequence impedance components are thus calculated by substituting the relevant terms of equations (4.13) – (4.18) by their corresponding values as obtained from standard tables ([13], [20]) and from Fig. 4.3. Thus, we get:

$$Z_1 = 1.1072 + j*0.33794\ \Omega/km, \text{ and } Z_0 = 2.08044 + j*1.48226\ \Omega/km \qquad (4.19)$$

The capacitance from phase to ground for a concentric neutral underground cable is given by [15]:

$$C_{\Phi\text{-}g} = (2*\prod*\varepsilon_o*\varepsilon_r)/(\log_e(DN_2/r_c) - ((1/n)*\log_e(n*r_n/DN_2))) \quad (4.20)$$

In equation (4.20), the terms 'DN_2', 'r_n' and 'n' are as described under equations (4.13) – (4.18), 'ε_o' is the permittivity of free space (8.854 nF/km), 'ε_r' is the relative permittivity for the TRXLPE insulation layer ($\varepsilon_r = 2.3$), and 'r_c' is the radius of the phase conductor (inches). Substituting all the relevant terms in equation (4.20) by their corresponding values, the phase-to-ground capacitance for the concentric neutral cable under consideration is found to be equal to 97.9 nF/km. Assuming that there is no mutual capacitance between the phases due to the presence of the insulation layers [15], the phase admittance matrix for the cable configuration of Fig. 4.3. is diagonal with all the leading diagonal terms being equal to $j*\omega*97.9$ $n\Omega^{-1}$/km. Performing a sequence admittance transformation [15] on the phase admittance matrix yields a diagonal sequence admittance matrix which is exactly the same as the phase admittance matrix. The sequence capacitance terms are therefore found to be equal to the phase-to-ground value calculated using equation (4.20). Thus, $C_1 = C_0 = 97.9$ nF/km.

4.3.2. Underground Cables, Single Phase

The single phase underground cables used in the electrical distribution network of Micropolis consist of seven strands of 2 AWG thick Al conductors, a 175 mils thick TRXLPE insulation layer, a "full" concentric neutral comprising of ten strands of 14 AWG thick Cu wires and a LLDPE encapsulating jacket. The impedance of single phase concentric neutral underground cables can be calculated using equations (4.13) – (4.18)

after substituting the term 'Z_{ab}' by 0. The phase-to-ground capacitance can then be calculated using equation (4.20). The impedance and capacitance values thus calculated are given as:

$$Z = 1.5075 + j*0.6055\ \Omega/km,\ C = 106.9\ nF/km \tag{4.21}$$

4.3.3. Overhead Lines, Three Phase, Single Circuit

It is assumed that all three phase, single circuit overhead lines present in the electrical distribution network of Micropolis have the same conductor configuration as that shown in Fig. 4.4. The primitive impedance matrix 'Z_{prim}' for this configuration is calculated as [16]:

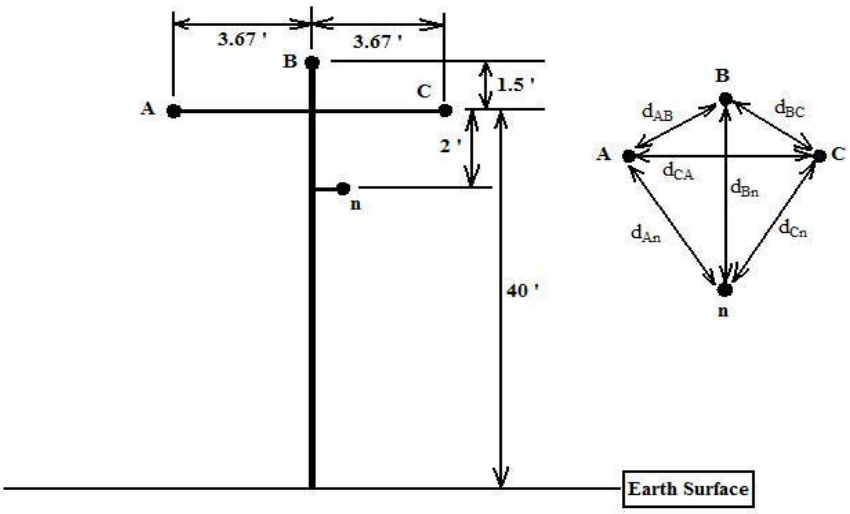

Fig. 4.4. Three phase, single circuit overhead line conductor configuration.

$$Z_{prim} = \begin{bmatrix} z_{aa} & z_{ab} & z_{ac} & z_{an} \\ z_{ba} & z_{bb} & z_{bc} & z_{bn} \\ z_{ca} & z_{cb} & z_{cc} & z_{cn} \\ z_{na} & z_{nb} & z_{nc} & z_{nn} \end{bmatrix} \tag{4.22}$$

$$z_{ii} = r_i + 0.0953 + j*0.12134*\log_e((1/GMR_i) + 7.934)\ \Omega/mi \quad (4.23)$$

$$z_{ij} = 0.0953 + j*0.12134*\log_e((1/GMD) + 7.934)\ \Omega/mi \quad (4.24)$$

While equation (4.23) is used to calculate the diagonal elements of matrix Z_{prim}, equation (4.24) is used to compute the off-diagonal terms. In equation (4.23), 'r_i' is the conductor resistance in ohms/mile and 'GMR_i' is the conductor geometric mean radius in feet (data available in standard tables, [13]). Assuming that all conductors are ideally transposed, the term 'GMD' in equation (4.24) is equal to $\sqrt[3]{d_{AB} * d_{BC} * d_{CA}}$ for all off-diagonal terms of matrix Z_{prim} involving any two phase conductors, and is equal to $\sqrt[3]{d_{An} * d_{Bn} * d_{Cn}}$ for all off-diagonal terms involving a phase conductor and the neutral (see Fig. 4.4). The [4X4] primitive impedance matrix is then reduced to a [3X3] phase impedance matrix 'Z_{abc}' using Kron reduction [16], as shown below:

$$Z_{abc} = \begin{bmatrix} Z_{aa} & Z_{ab} & Z_{ac} \\ Z_{ba} & Z_{bb} & Z_{bc} \\ Z_{ca} & Z_{cb} & Z_{cc} \end{bmatrix} \quad (4.25)$$

$$Z_{ij} = z_{ij} - (z_{in}*z_{nj})/z_{nn} \quad (4.26)$$

The elements of matrix Z_{abc} can be computed using equation (4.26), where the terms to the right hand side of the equation refer to those of the matrix Z_{prim}. Once Z_{abc} has been calculated, a sequence impedance transformation is then performed on it in order to obtain the [3X3] sequence impedance matrix 'Z_{012}' as shown below [16]:

$$Z_{012} = [A^{-1}]*Z_{abc}*A \quad (4.27)$$

$$A = \begin{bmatrix} 1 & 1 & 1 \\ 1 & a^2 & a \\ 1 & a & a^2 \end{bmatrix} \quad (4.28)$$

In equation (4.28), the operator 'a' represents the complex quantity $e^{j*(2*\Pi/3)}$. The calculated sequence impedance matrix has the following diagonal structure, where 'Z_0' represents the zero sequence impedance of the concerned overhead line and 'Z_1' the positive sequence impedance.

$$Z_{012} = \begin{bmatrix} Z_0 & 0 & 0 \\ 0 & Z_1 & 0 \\ 0 & 0 & Z_2 \end{bmatrix} \tag{4.29}$$

For calculating the sequence capacitance values for three phase overhead lines, the first step is to form the [4X4] potential coefficient matrix 'P_{pot}' as shown below [14]:

$$P_{pot} = \begin{bmatrix} p_{aa} & p_{ab} & p_{ac} & p_{an} \\ p_{ba} & p_{bb} & p_{bc} & p_{bn} \\ p_{ca} & p_{cb} & p_{cc} & p_{cn} \\ p_{na} & p_{nb} & p_{nc} & p_{nn} \end{bmatrix} \tag{4.30}$$

$$p_{ii} = (1/(2*\Pi*\varepsilon_o))*\log_e(2*h_i/r_i) \text{ km/nF} \tag{4.31}$$

$$p_{ij} = (1/(2*\Pi*\varepsilon_o))*\log_e(D_{ij}/d_{ij}) \text{ km/nF} \tag{4.32}$$

While equation (4.31) is used to calculate the diagonal elements of matrix P_{pot}, equation (4.32) is used to compute the off-diagonal terms. In equation (4.31), 'h_i' represents the average height above ground (feet) of conductor 'i' (see Fig. 4.4); while 'r_i' is the conductor radius in feet (data available in standard tables, [13]). In equation (4.32), 'D_{ij}' is the distance in feet between the conductor 'i' and the image below earth surface of the conductor 'j', and 'd_{ij}' is the distance in feet between the conductors 'i' and 'j' (see Fig. 4.4). 'ε_o' is the permittivity of free space and is equal to 8.854 nF/km. The [4X4] potential coefficient matrix is then reduced to a [3X3] matrix 'P_{red}' using the Kron reduction formula as given in equation (4.26). The capacitance matrix 'C_{red}' is then

obtained by inverting matrix P_{red}. Thus, $C_{red} = [P_{red}]^{-1}$ (nF/km). Finally, the sequence capacitance values are computed by performing a sequence admittance transformation on the matrix C_{red}, using the same procedure as was outlined through equations (4.27) – (4.28). Thus,

$$C_{012} = [A^{-1}]*C_{red}*A \tag{4.33}$$

Table 4.2 shows the calculated sequence impedance and capacitance values associated with the different three phase overhead lines present in the electrical distribution network of Micropolis.

TABLE 4.2
SEQUENCE IMPEDANCE AND CAPACITANCE VALUES FOR THREE PHASE SINGLE CIRCUIT OVERHEAD LINES

Conductor Size	**Z_1 (Ω/km)**	**Z_0 (Ω/km)**	**C_1 (nF/km)**	**C_0 (nF/km)**
6 AWG	2.6411 + j*0.5102	3.0341 + j*1.803	8.6643	4.6495
2 AWG	1.0433 + j*0.4762	1.5173 + j*1.4968	9.3391	4.9021
3/0 AWG	0.4134 + j*0.4411	0.7597 + j*1.1775	10.131	5.1929
4/0 AWG	0.3281 + j*0.432	0.6285 + j*1.1261	10.354	5.2741
266.8 kcmil	0.2602 + j*4235	0.5171 + j*1.0858	10.5836	5.3569
397.5 kcmil	0.1752 + j*0.4044	0.3702 + j*1.0259	11.0303	5.5173

4.3.4. Overhead Lines, Single Phase

It is assumed that all single phase overhead lines of the electrical distribution network of Micropolis have the same conductor configuration as that shown in Fig. 4.5. The value of the conductor resistance (Ω/km) is obtained from standard tables as given in [19]. The inductance per conductor and the capacitance across the conductors of Fig. 4.5 are calculated as ([21] – [22]):

$$L_{\Phi} = 0.2*\log_e(GMD/GMR) \text{ mH/km, and } C_{\Phi\text{-}n} = 1/(36*\log_e(D/r)) \ \mu\text{F/km} \tag{4.34}$$

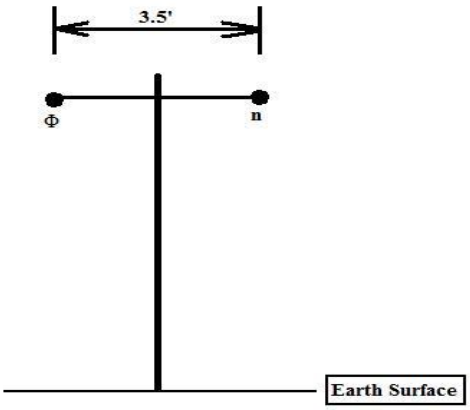

Fig. 4.5. Single phase overhead line conductor configuration.

In equation (4.34), 'GMR' is the conductor's geometric mean radius expressed in feet, 'r' is the physical radius of the conductor expressed in feet (data available in standard tables, [13]), and 'D' is the distance of separation (feet) between the conductors. Assuming that both the phase and the neutral conductors have the same cross-section area and number of strands, the term 'GMD' in equation (4.34) is approximately equal to the distance of separation between the two conductors [13]. Table 4.3 shows the calculated resistance, inductance and capacitance values associated with the different single phase overhead lines present in the electrical distribution network of Micropolis.

TABLE 4.3
RESISTANCE, INDUCTANCE AND CAPACITANCE VALUES FOR SINGLE PHASE OVERHEAD LINES

Conductor Size	**R (Ω/km)**	**L (mH/km)**	**C (nF/km)**
6 AWG	2.6411	1.2876	4.5362
2 AWG	1.0433	1.1972	4.9062

4.3.5. Overhead Lines, Three Phase, Double Circuit

The distribution feeders of Micropolis run in a double circuit configuration for some distance after emanating from the substation, before branching off into their respective service areas. The concerned configuration is as shown in Fig. 4.6. The calculation of the sequence impedance and capacitance values for this configuration follows the same steps as were explained in Section 4.3.3 [15].

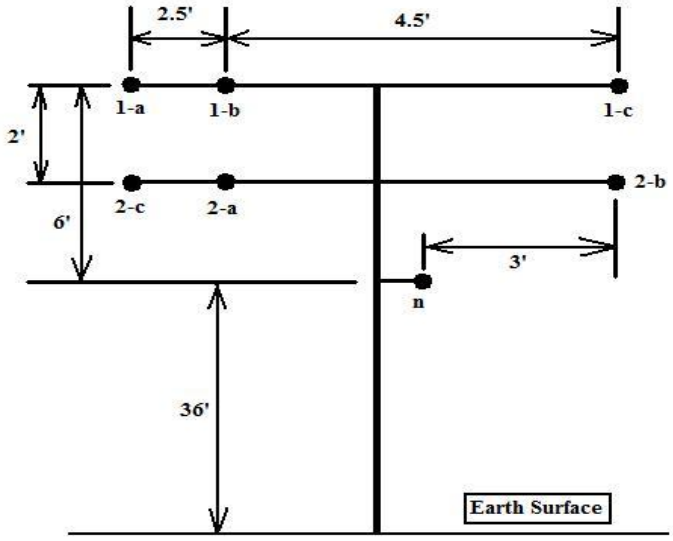

Fig. 4.6. Three phase, double circuit overhead line conductor configuration.

As can be observed from Fig. 4.6, the primitive impedance matrix 'Z_{prim}' for this situation would be of the order [7X7]. The primitive impedance matrix is then reduced to a [6X6] phase impedance matrix '$Z_{abc,12}$' using the Kron reduction formula as given in equation (4.26). The matrix $Z_{abc,12}$ has the following structure:

$$Z_{abc,12} = \begin{bmatrix} Z_{1a,1a} & Z_{1a,1b} & Z_{1a,1c} & | & Z_{1a,2a} & Z_{1a,2b} & Z_{1a,2c} \\ Z_{1b,1a} & Z_{1b,1b} & Z_{1b,1c} & | & Z_{1b,2a} & Z_{1b,2b} & Z_{1b,2c} \\ Z_{1c,1a} & Z_{1c,1b} & Z_{1c,1c} & | & Z_{1c,2a} & Z_{1c,2b} & Z_{1c,2c} \\ - & - & - & + & - & - & - \\ Z_{2a,1a} & Z_{2a,1b} & Z_{2a,1c} & | & Z_{2a,2a} & Z_{2a,2b} & Z_{2a,2c} \\ Z_{2b,1a} & Z_{2b,1b} & Z_{2b,1c} & | & Z_{2b,2a} & Z_{2b,2b} & Z_{2b,2c} \\ Z_{2c,1a} & Z_{2c,1b} & Z_{2c,1c} & | & Z_{2c,2a} & Z_{2c,2b} & Z_{2c,2c} \end{bmatrix} \quad (4.35)$$

The matrix $Z_{abc,12}$ is then partitioned as shown in equation (4.35) in order to yield four [3X3] matrices. While the phase impedance matrix corresponding to line 1in Fig. 4.6 is obtained by the partitioning of the first three rows and columns, the phase impedance matrix for line 2 is obtained by the partitioning of the last three rows and columns. The other two partitioned matrices represent the mutual coupling between the two lines. The sequence impedance components corresponding to a given line is then obtained by performing a sequence impedance transformation, as given in equations (4.27) – (4.28), on the partitioned phase impedance matrix corresponding to that line.

Similarly, for calculating the sequence capacitance values for the configuration of Fig. 4.6, we first form the [7X7] potential coefficient matrix 'P_{pot}' as outlined in Section 4.3.3. The matrix P_{pot} is then reduced to a [6X6] matrix '$P_{red,12}$' using the Kron reduction formula as given in equation (4.26). The capacitance matrix '$C_{red,12}$' is thereafter obtained by inverting the matrix $P_{red,12}$. Thus, $C_{red,12} = [P_{red,12}]^{-1}$ (nF/km). The [6X6] capacitance matrix $C_{red,12}$ is then partitioned as explained above in order to yield four [3X3] matrices. The sequence capacitance values associated with each line of Fig. 4.6 are then obtained by performing a sequence admittance transformation on the [3X3] capacitance matrix corresponding to the concerned line.

The different sequence impedance and capacitance values thus calculated for the three phase, double circuit overhead lines present in the electrical distribution network of Micropolis are as shown in Table 4.4.

TABLE 4.4
SEQUENCE IMPEDANCE AND CAPACITANCE VALUES FOR THREE PHASE DOUBLE CIRCUIT OVERHEAD LINES

	Conductor Size	**Z_1 (Ω/km)**	**Z_0 (Ω/km)**	**C_1 (nF/km)**	**C_0 (nF/km)**
Line 1	397.5 kcmil	0.1752 + j*0.3948	0.3532 + j*1.1693	11.7681	7.5193
Line 2	266.8 kcmil	0.2602 + j*4138	0.4475 + j*1.1187	11.2772	7.8502

4.3.6. Overhead Lines, Two Phase

It is assumed that all two phase overhead lines of the electrical distribution network of Micropolis have the same conductor configuration as that shown in Fig. 4.7. As can be observed from the figure, the primitive impedance matrix for this situation would be of the order [3X3] as shown below [15]:

$$Z_{prim} = \begin{bmatrix} z_{aa} & z_{ac} & z_{an} \\ z_{ca} & z_{cc} & z_{cn} \\ z_{na} & z_{nc} & z_{nn} \end{bmatrix} \tag{4.36}$$

The primitive impedance matrix of equation (4.36) is then reduced to a [2X2] phase impedance matrix 'Z_{ac}' using the Kron reduction formula as given in equation (4.26). The [3X3] 'phase frame' matrix 'Z_{abc}' is then constructed from Z_{ac} by filling in '0's for the missing phase as shown [15]:

$$Z_{abc} = \begin{bmatrix} Z_{aa} & 0 & Z_{ac} \\ 0 & 0 & 0 \\ Z_{ca} & 0 & Z_{cc} \end{bmatrix} \tag{4.37}$$

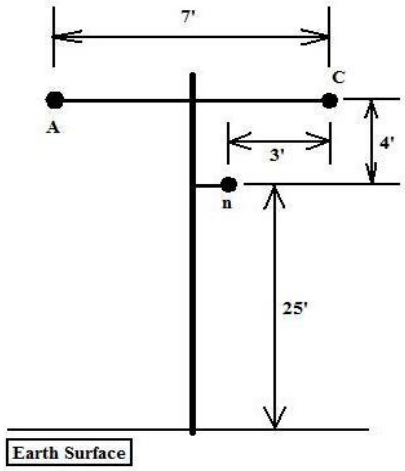

Fig. 4.7. Two phase overhead line conductor configuration.

The sequence impedance components are then calculated by performing a sequence impedance transformation on Z_{abc}, as explained using equations (4.27) – (4.28).

The sequence capacitance terms are calculated by first forming the [3X3] potential coefficient matrix 'P_{pot}' corresponding to the configuration of Fig. 4.7. The matrix P_{pot} is then reduced to a [2X2] matrix '$P_{red,ac}$' using the Kron reduction formula as given in equation (4.26). The capacitance matrix '$C_{red,ac}$' is thereafter obtained by inverting the matrix $P_{red,ac}$. Thus, $C_{red,ac} = [P_{red,ac}]^{-1}$ (nF/km). The [3X3] 'phase frame' matrix '$C_{red,abc}$' is then constructed from $C_{red,ac}$ by filling in '0's for the missing phase as shown:

$$C_{red,abc} = \begin{bmatrix} C_{aa} & 0 & C_{ac} \\ 0 & 0 & 0 \\ C_{ca} & 0 & C_{cc} \end{bmatrix} \tag{4.38}$$

The sequence capacitance terms are then obtained by performing a sequence admittance transformation on $C_{red,abc}$, as explained using equation (4.33). The sequence

impedance and capacitance values thus calculated for the configuration of Fig. 4.7 are given as:

$$Z_1 = 1.8021 + j*0.4941\ \Omega/km, \text{ and } Z_0 = 1.9263 + j*0.9011\ \Omega/km \quad (4.39)$$

$$C_1 = 5.0289\ nF/km, \text{ and } C_0 = 3.7739\ nF/km \quad (4.40)$$

4.4. Formulation of Protection Scheme for Electrical Test Bed

The layout of the electrical distribution network of Micropolis is as shown in Fig. 4.8. Defining a 'Line' as a switchable section of the network formed by one or more isolating elements at its ends, one may observe from Fig. 4.8 how a faulted Line can be isolated by opening its corresponding terminating isolators. Since Micropolis is a small city covering an area of approximately 2 square miles, it is assumed that all isolators present in the distribution system are manually operated. The utility personnel thus typically rely on customer calls in order to locate a particular fault, before isolating it physically and carry out repair and restoration services.

The substation breakers of the distribution network, however, are assumed to be operated through over-current relays. In the event that a short circuit fault occurs at some point in the distribution system, the relay trips the breaker open. After a sufficient delay during which the maintenance personnel are assumed to have located and isolated the concerned fault, the breaker is closed in order to restore service to the remaining parts of the network. This logic is implemented in the test bed using the relay module of Fig. 4.9 ([17] – [18]). As can be observed from the figure, the instantaneous values of the phase currents are first converted to their corresponding r.m.s values before being compared to

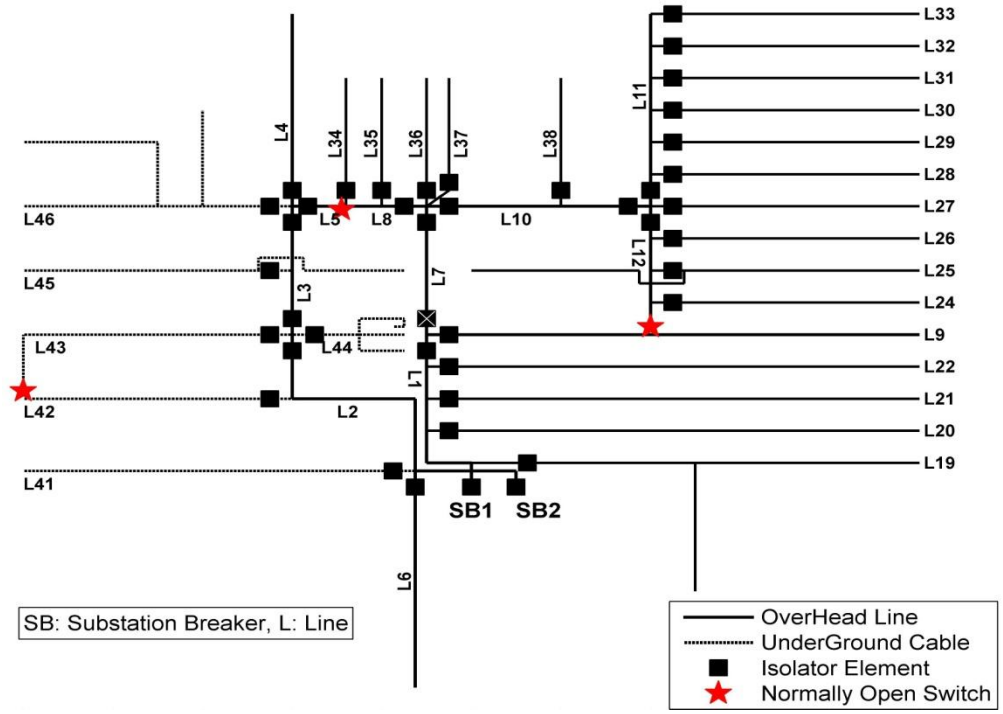

Fig. 4.8. Layout of the power distribution network for the city of Micropolis.

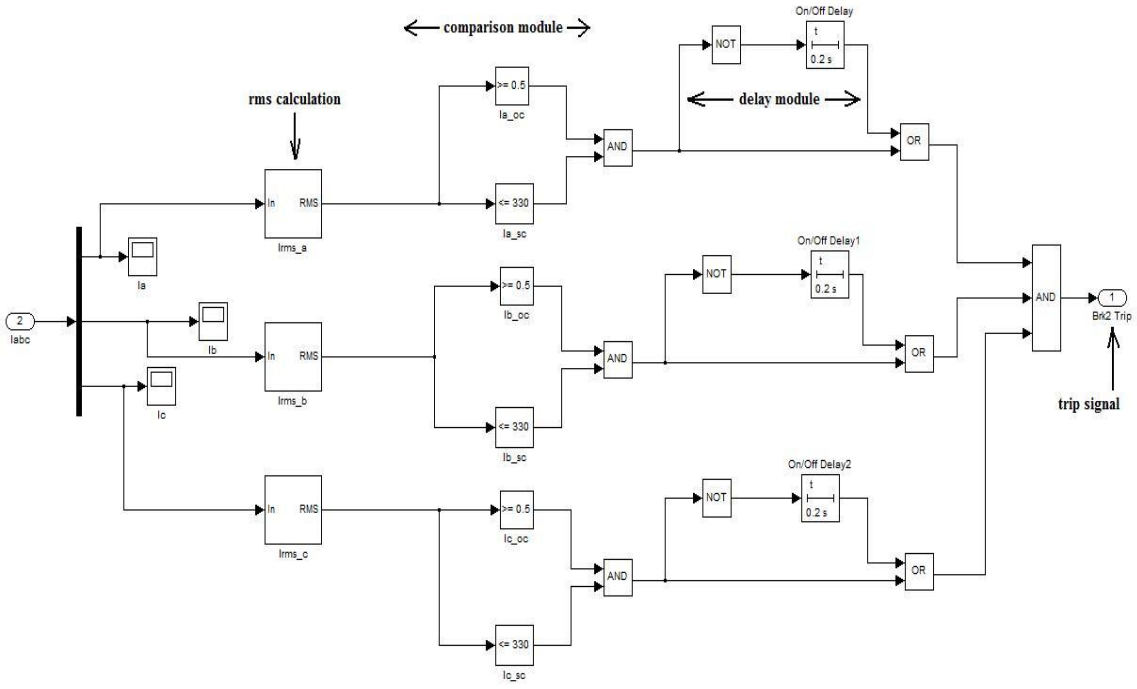

Fig. 4.9. Snapshot of the three phase over-current relay module.

prefixed bounds in the ‘comparison module’. While the upper bound corresponds to 1.5 times the r.m.s value of the nominal phase current under normal operating conditions of the system, the lower bound is equal to a current level of 0.5 A (any small positive value will do). Thus, under normal operating conditions, the r.m.s values of the phase currents satisfy these boundary conditions and hence the output of the corresponding ‘AND’ blocks are all ‘1’. The ‘OR’ blocks at the end of the ‘delay module’ thus all output ‘1’ such that the breaker trip signal is ‘1’ as well (corresponding to breaker being closed).

Assuming that a phase A-to-ground short circuit fault now occurs at some point in the distribution system, the r.m.s value of the phase A fault current exceeds the upper bound, and hence the output of the corresponding ‘AND’ block becomes ‘0’. The ‘On/Off Delay’ block operates in the following fashion. It normally outputs a ‘0’ signal, but when its input changes from ‘0’ to ‘1’; its output becomes ‘1’ after a specified time delay as long as its input is still ‘1’. Thus, under normal operating conditions of the system, when the ‘AND’ blocks at the end of the comparison module all output ‘1’, the inputs to the on/off delay blocks through the ‘NOT’ gates are all ‘0’. When the above mentioned fault occurs, the ‘AND’ block corresponding to phase A outputs a ‘0’, so that the corresponding delay block sees a ‘1’ at its input. At this time, since the outputs of the ‘AND’ and the delay block for phase A are both ‘0’, the corresponding ‘OR’ block outputs a ‘0’ as well, so that the relay trips the breaker open.

Once the breaker opens, the system current falls to 0, and hence the r.m.s. values of all the phase currents now drop below their corresponding lower bounds. The outputs of the ‘AND’ blocks at the end of the comparison module are therefore all held at ‘0’. As

a result, the on/off delay blocks still see a ‘1’ at their inputs after the specified delay period (which corresponds to the time the utility personnel take in manually clearing the concerned fault) is over, and hence they output a ‘1’ at this time. This is turn causes the outputs of the corresponding ‘OR’ blocks to become ‘1’, and hence the breaker trip signal is ‘1’ as well. The breaker is thus closed again in order to restore service to the healthy parts of the electrical network.

4.5. Assigning of System Loads

For simplicity sake, the various users across Micropolis have been categorized into different profiles (e.g. residential, commercial, industrial etc.), and it is assumed that the customers belonging to each such profile have a fixed load demand (KVA) all through the year. The different load profiles are as shown in Table 2.1. It is further assumed that the local electric utility maintains a constant power factor of 0.95 for all load points across the city. Thus, all buildings connected to a given distribution transformer are modeled in the test bed as a single load point with a fixed KW and KVAR demand associated with it.

4.6. Source of Power Supply

Though it was mentioned in Chapter II that Micropolis does not have a power generation facility of its own owing to its small size, a three phase voltage source rated at 138 KV (the rating of the sub-transmission line) has been added to the test bed as a source of power for the entire distribution network.

4.7. Conclusion

Though it was originally planned to use this test bed for running the fire spread simulations on the electrical distribution network of Micropolis, the excessive time required to complete any given simulation run was a major deterrent to this approach. The fire spread studies were therefore carried out using an alternative methodology as proposed in the subsequent chapters. This test bed, however, might still prove to be helpful for researchers who wish to carry out any form of electrical analysis (e.g. short circuit analysis, power flow studies, etc.) of the distribution system, as a part of studying the effects of disasters on the interconnected infrastructure components of a city.

CHAPTER V

METHODOLOGY USED FOR ELECTRICAL SIMULATION RUNS

As mentioned in Chapter IV, since the original plan of using the Simulink based test bed for carrying out the fire spread studies on the electrical distribution network of Micropolis was abandoned, an alternative approach was devised as described in this and the subsequent chapters. Though the proposed methodologies and algorithms have been explained using the example of Micropolis, they are quite general in scope and can be easily implemented on any given distribution network.

This chapter describes how we can use the fire polygon vertex coordinates output by the MUFS code for studying and quantifying the damage caused by a given fire spread scenario to the electrical network. The following sections discuss all relevant assumptions, definitions and algorithms pertaining to the formulation and the implementation of the proposed methodology [8].

5.1. Assumptions

1) We are dealing with a radial distribution system.

2) Though there are three Normally Open switches located across the electrical distribution network of Micropolis (as shown in Fig. 4.8), they are assumed to be non-functional for the time being.

3) The Micropolis electrical distribution system is assumed to be connected to an infinite bus, so that events like a sudden loss of system load does not cause any system stability issues.

4) Since fire spreads along the ground, its effect on the electrical system can be accounted for by considering the status of only two types of electrical components: poles and pad-mounted transformers.

5) Any pole or pad-mounted transformer which is found to be partially or fully enclosed inside the fire polygon area for a given time step is considered to be faulted.

6) Repair and restoration of electrical components is not being considered during fire spread.

7) Since the fire spread duration of 12 hours is only a small fraction of the Mean Up Time of an electrical component, it is assumed that all faults occurring during the course of a given simulation are a result of the fire only.

5.2. Definitions of Important Terms

1) Line: A 'Line' is a switchable section of the electrical network formed by one or more isolating element(s) at its ends. The location of the isolators and the nomenclature of the Lines (as shown in Fig. 4.8) are purely a matter of system design. For any given Line, its 'upstream' end is the one through which power flows into it; the other end being the 'downstream' end.

2) Isolator Bank: An 'Isolator Bank' (or just a 'Bank') is a point in the distribution network where a three-phase section of the feeder branches off into two or more three-phase sub-branches. The intersection point of Lines 1, 9 and 7 in Fig. 4.8 is an example of a Bank.

3) Upstream vs. Downstream: A component 'X' is said to be 'upstream' with respect to a component 'Y' if X is electrically closer to the substation than Y. In other

words, if we trace a path joining the substation to X and Y such that we move along the flow of power, we shall come across X first and then Y.

5.3. General Treatment of Faulted Components

Under assumptions 4 and 5 (see Section 5.1), if a pole or a pad-mounted transformer is found to be enclosed inside the fire polygon area for a given simulation time step, the concerned component is then isolated from the rest of the network using the following methodology [8].

5.3.1. Faulted Pole

If a pole belonging to any Line is found to be faulted, the concerned Line is isolated irrespective of the type of the fault (short or open circuit). This is done taking into consideration the fact that even though the fault might just be a local open circuit, the fire will eventually cause the wooden poles to crumble down along with the overhead conductors mounted on them. The isolation of the Line thus ensures that there are no live wire ends present on the ground during the time when people are being evacuated from the fire spread area. If, however, the affected pole represents a Bank, it is isolated by opening the ‘upstream’ end isolator of the Line which is immediately upstream with respect to the Bank. For example, assuming that the Bank represented by the intersection point of Lines 7, 8 and 10 in Fig. 4.8 gets faulted, it is isolated by opening the isolator of Line 7 represented by the filled black square with a white cross marked across it.

5.3.2. Faulted Pad-Mounted Transformer

On the lines of the approach proposed in subsection 5.3.1, if a pad-mounted transformer belonging to any Line is found to be faulted, the concerned Line is isolated as well. Since pad-mounted transformers are enclosed in iron casings, there is an enormous build-up of gas and soot particles inside the casing once the fire engulfs it. Leaving a high voltage live wire end in the casing can cause the gas to get ionized and may even result in some dangerous blasts.

5.4. Load Loss Damage Index (LLDI)

Distribution system reliability indices like SAIDI, SAIFI, and CAIDI [23] are generally used by electric utilities for planning and operational purposes. A closer look at the indices, however, reveals that these are all average values calculated using data collected from the observation of the system over a pre-defined period of time (usually annually). As mentioned earlier, since the focus of this research is only on the window of time during which the fire spreads, these indices are not really suitable for this study.

An alternative, the Load Loss Damage Index (LLDI), is therefore being proposed and defined as [8]:

$$\text{LLDI} = \sum_{i=1}^{T/t} \text{KVA}_i * (T - t * i)\ \text{KVAh} \tag{5.1}$$

In equation (5.1), 'KVA_i' represents the total load (in KVA) lost in simulation time step 'i' due to the isolation of faulted Lines and/or Banks. The terms 't' and 'T' respectively represent the total duration (in hours) of the physical fire spread which one time step and one complete run of the MUFS simulation corresponds to. As mentioned in Chapter III, the relevant values of 't' and 'T' are equal to 1/12 hours (5 minutes) and

12 hours respectively. The expression within the parenthesis of equation (5.1) therefore represents the time (in hours) left till the end of simulation, with respect to the current time step. The LLDI value (in KVAh) thus calculated can therefore be used to measure the extent of the damage caused to the electrical network for a given fire spread scenario.

5.5. Electrical Simulation Algorithm

Keeping in mind the assumptions and the general methods of treatment of faulted components as proposed in the earlier sections, the electrical simulations are run using the following algorithm [8].

1) Read the fire polygon coordinates for a given time step from the MUFS output files.

2) Determine which all poles and/or transformers are fully or partially enclosed inside the fire spread area for the given time step. Note that the fire polygon and the individual pole and transformer coordinates all conform to the GIS layout of Micropolis in ArcMap (see Chapter II).

3) Determine all Lines and/or Banks that are affected by the faulted poles and/or transformers as found in step (2).

4) Scan all Line/Bank numbers as found in step (3) to determine which of those are downstream with respect to the others. Eliminate all such downstream Line/Bank numbers from the list of (3) as they will anyways be getting isolated by the isolation of their concerned upstream components.

5) Isolate each of the upstream Lines/Banks as identified in step (4). For each such isolated upstream component, scan all Lines/Banks which are located downstream

with respect to it. If any of such downstream Lines/Banks is found to be live till now, it will also get ‘effectively isolated’ as a result of the isolation of the concerned upstream component.

6) For each Line/Bank getting physically or effectively isolated in the current time step, calculate the total load (KVA) lost as a result of such outages.

7) Are all upstream Lines/Banks as found in step (4) isolated? If yes, go to (8). If not, go to (5).

8) Calculate the current time step’s contribution to the LLDI using equation (5.1).

9) Check if the MUFS simulation has been completed (entire 12 hours of simulation data has been generated) OR if both the substation breakers of Micropolis have been opened (in which case, the city has been blacked out). If either of the conditions is satisfied, end simulation and print results. Else, increase iteration count and go to step (1).

The above mentioned algorithm is then used to implement the methodology proposed in this chapter for studying and quantifying the damage caused by fire to the electrical network. The following chapter discusses all relevant results obtained from running numerous simulations on the Micropolis distribution system, corresponding to different fire spread scenarios.

CHAPTER VI

ANALYSIS OF ELECTRICAL SIMULATION RUNS

This chapter presents the results [8] obtained from running numerous simulations on the electrical distribution network of Micropolis, corresponding to different fire spread scenarios. A close look at Tables 3.1 and 3.2 indicates that with the different numbers of supporting infrastructure damage profiles, urban fire ignition point profiles and wind directions considered for the purpose of this research, a total of 10*4*4 = 160 different fire spread scenarios can be generated. The various conclusions drawn from these simulation runs have been arranged in the following two categories.

6.1. Most Damaging SIDP

Ten different simulations corresponding to the various supporting infrastructure damage profiles were run for a given UFIP and wind direction combination. The LLDI values calculated for all such simulation runs were then compared to determine the worst infrastructure damage profile. The results of all relevant simulation runs are as shown in Figs. 6.1(a) – (d). The following conclusions can be drawn from these figures [8].

1) Damage Profile AD1, which simulates the simultaneous destruction of all three high-service pumps and the elevated storage tank, is by far the most damaging profile across all different wind direction and UFIP combinations. This is natural as the water pressure at the fire hydrants is seriously affected due to the unavailability of both the storage tank and the high-service pumps. The fire thus spreads rapidly and this leads

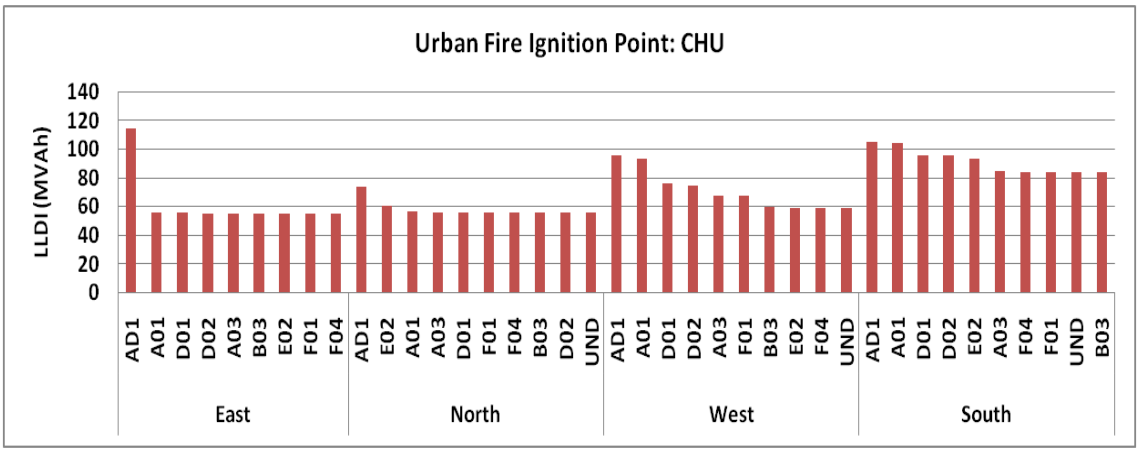

(a)

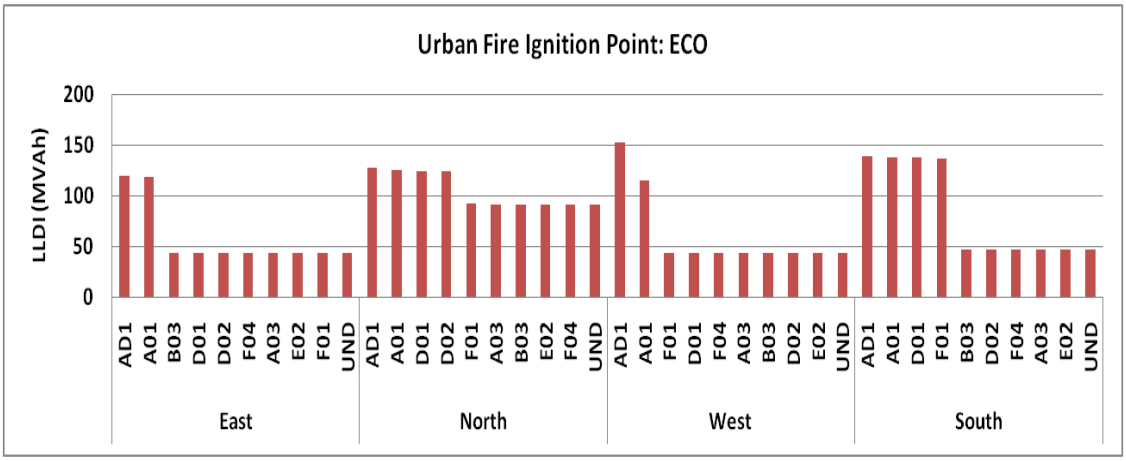

(b)

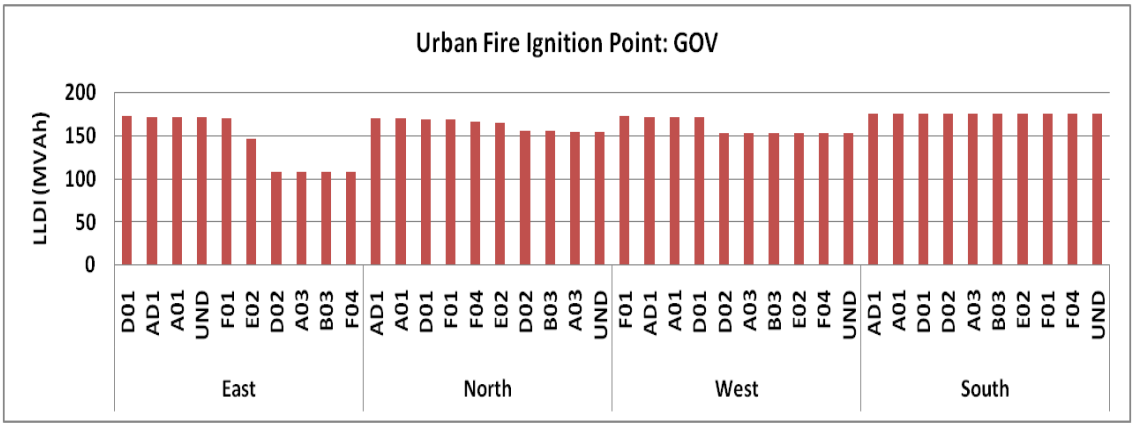

(c)

Fig. 6.1. Results of electrical simulations run using MUFS data.

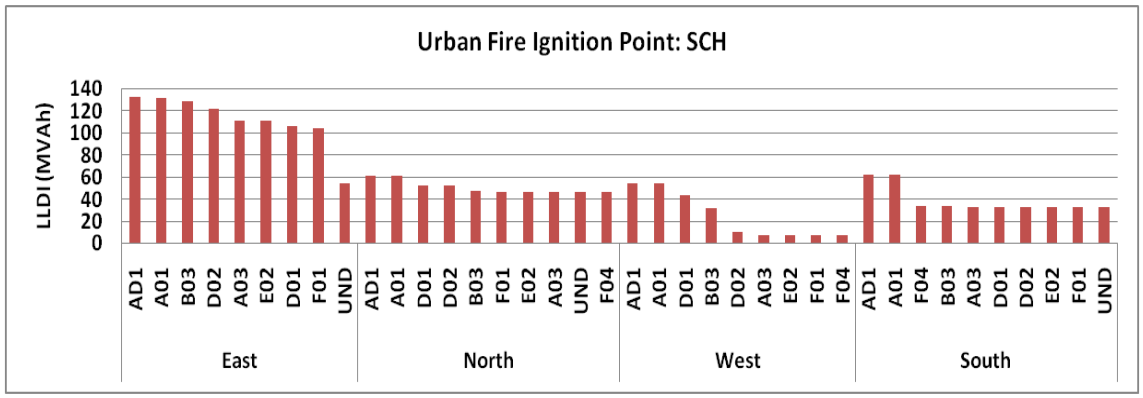

(d)

Fig. 6.1. continued.

to the outage of more Lines/Banks in the earlier stages of the simulation, thereby yielding a high LLDI value.

2) The next most damaging profiles can be mostly found to be those of A01 and D01. While A01 is a subset of AD1, the interesting thing to note about D01 is that its LLDI value is mostly higher than that of D02. The reason for this is that while in the case of D01 the storage tank is unavailable for the entire duration of simulation, it is assumed to be available during the first hour of fire spread in the case of D02. The fire is thus better contained towards the beginning of the simulation for D02, leading to less electrical outages and hence a lower LLDI value.

3) As expected, the LLDI value for the UND profile is usually the least, as it does not simulate the damage of any supporting infrastructure for fire response. Thus, the fire fighters have better resources to contain the fire, leading to less electrical outages.

4) Damage Profiles A03 and B03, which are really a subset of profile A01, can be found to be having significantly lower LLDI values than that of A01.

5) Though the LLDI values for profiles E02, F01 or F04 are generally found to be on the lower side, they have a greater degree of variation with respect to the different wind direction and UFIP combinations. This is probably because these profiles do not have any significant impact on the fire suppression efforts.

Note that the LLDI values corresponding to three out of the above mentioned 160 different fire spread scenarios are missing from the Figs. 6.1(a) – (d). This is either because MUFS generated some run-time errors while simulating such scenarios, or because the data required for such simulation runs was unavailable. Also, the LLDI value for damage profile UND (GOV, East) is found to be exceptionally high. The LLDI value, however, just reflects the typical pattern of the fire polygon coordinates as output by the MUFS code for that simulation. These four cases account for just 2.5% of the total simulations run, and can therefore be safely ignored.

6.2. Most Damaging UFIP

Table 6.1 shows the average LLDI values calculated over all combinations of SIDPs and wind directions for a given UFIP profile. As can be seen, the two most damaging ignition point profiles turn out to be those comprising of the city's government buildings and the ecological targets respectively [8].

Referring to Fig. 2.1, where the government buildings had been represented by a 'G' marked on them, one may note their proximity to the city's central business district, the industrial area and the two feeders coming out of the city's substation. Thus, a fire

starting from these buildings causes a heavy loss of load in the early stages of the simulations, thereby yielding high LLDI values.

TABLE 6.1
MOST DAMAGING UFIP

Ignition Point Acronym	Average LLDI value (MVAh)
GOV	160.811
ECO	76.845
CHU	70.889
SCH	55.909

The city's ecological targets, on the other hand, comprise of buildings containing highly inflammable materials. It is therefore quite obvious that a fire starting from them will be spreading very fast and will be difficult to contain, thereby leading to more electrical outages and a higher average LLDI value.

The results presented in this chapter are based on the principal assumption that the Normally Open (NO) switches present in the electrical distribution network of Micropolis are unavailable. Thus, routing of power during emergencies is not possible under this configuration. Electric power utilities, however, typically have numerous NO switches located at strategic points across the distribution network for reliability purposes. The following chapter proposes a methodology for routing power across faulted sections of the electrical network at times of emergencies. The proposed methodology is then implemented by means of an algorithm.

CHAPTER VII

GRAPH THEORY APPLICATIONS FOR ROUTING OF POWER DURING EMERGENCIES

Assuming that some parts of the electrical distribution network of a city have been faulted and subsequently isolated due to fire, this chapter presents a graph theoretic approach [24] for routing power across the isolated sections using a given set of NO switches. The routing is so done that the power flows along a path of minimum impedance. The following sections illustrate the proposed approach along with its associated algorithms using the example of Micropolis.

7.1. Assumptions

Since the methodology proposed in this chapter is basically an extension of the one presented in Chapter V, all assumptions listed in Section 5.1 hold for this approach as well, except for the second one. Figure 7.1 shows the layout of the electrical distribution network of Micropolis along with the three NO switches located at strategic points across it. It is assumed that all three of them are of the Triple Pole Single Throw (3PST) type [25].

7.2. General Treatment of Faulted Components

Under assumptions 4 and 5 of Section 5.1, if an electrical component (a pole or a pad-mounted transformer or a NO switch) is found to be enclosed inside the fire polygon area for a given simulation time step, it is then isolated from the rest of the network using the following methodology. Though the approaches described in this section are

very similar to those presented in Section 5.3, there are however some differences which are highlighted through the following subsections [24].

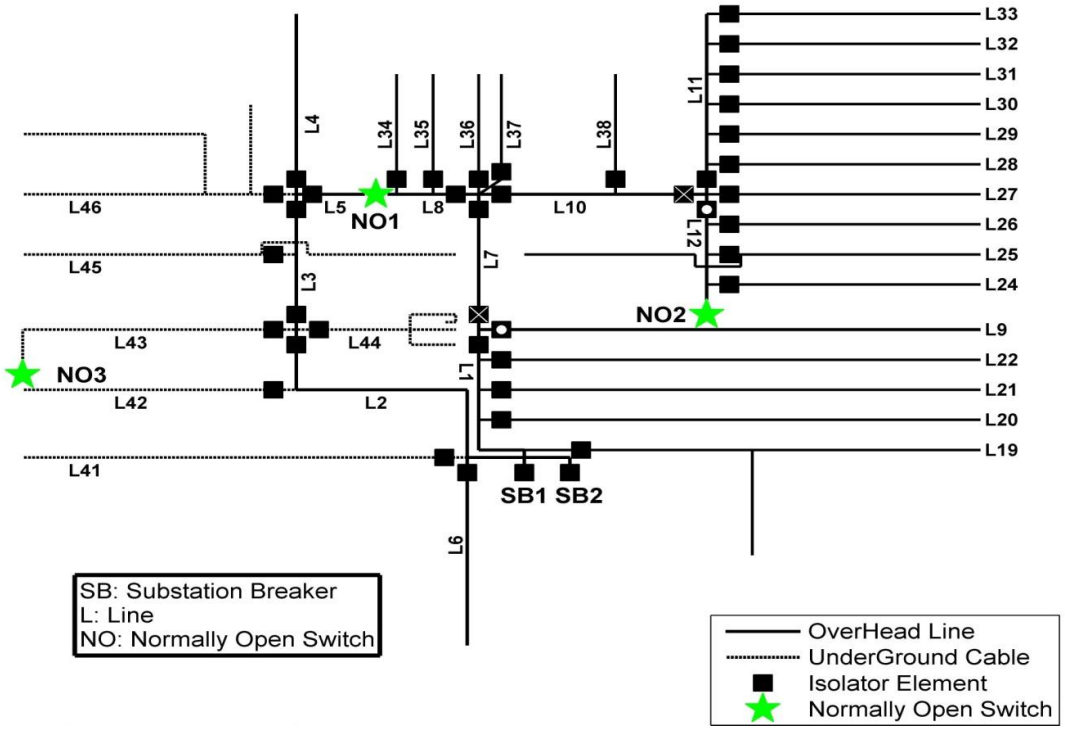

Fig. 7.1. Layout of the electrical distribution network of Micropolis.

7.2.1. Faulted Pole

If a pole belonging to any Line (see definition in Section 5.2) is found to be faulted, the concerned Line is isolated irrespective of the type of the fault (short or open circuit). This is done taking into consideration the fact that even though the fault might just be a local open circuit, the fire will eventually cause the wooden poles to crumble down along with the overhead conductors mounted on them. The isolation of the Line thus ensures that there are no live wire ends present on the ground during the time when

people are being evacuated from the fire spread area. If, however, the affected pole represents a Bank, it is isolated by opening the terminating isolators of the Lines incident at the Bank; such that the isolators themselves are not located at the Bank. If any of such terminating isolators happens to be a NO switch, it also has to be permanently opened in order to isolate the faulted Bank. For example, assuming that the Bank represented by the intersection point of Lines 7, 8 and 10 in Fig. 7.1 gets faulted, it is isolated by permanently opening the NO switch 1 and by opening the isolators of Lines 7 and 10 represented by the filled black squares with a white cross marked across them.

7.2.2. Faulted Pad-Mounted Transformer

On the lines of the approach proposed in subsection 7.2.1, if a pad-mounted transformer belonging to any Line is found to be faulted, we again isolate the concerned Line. Since pad-mounted transformers are enclosed in iron casings, there is an enormous build-up of gas and soot particles inside the casing once the fire engulfs it. Leaving a high voltage live wire end in the casing can cause the gas to get ionized and may even result in some dangerous blasts.

7.2.3. Faulted NO Switch

The NO switches located across the electrical network of Micropolis are assumed to be either pole or pad mounted, depending on whether they span across two overhead lines or two underground cables. Now, during the course of the electrical simulations, if it is determined that a pole or a pad containing a given NO switch is under fire, it can be isolated by opening the terminating isolators of the Lines across which the switch is physically present; such that the isolators themselves are not located at the site of the

switch. For example, assuming that the pole on which NO switch 2 is mounted (see Fig. 7.1) gets faulted, it is isolated by opening the isolators of Lines 9 and 12 represented by the filled black squares with a white circle marked on them.

7.3. Overall Electrical Simulation Algorithm

This section presents an extension of the algorithm of Section 5.5, by incorporating in it the concept of power routing during emergencies. The following algorithm [24] calls a subroutine, which in turn implements a graph theoretic approach (see Section 7.4) for routing power across faulted sections of the electrical network using a given set of NO switches.

1) Read the fire polygon vertex coordinates for a given time step from the MUFS output files.

2) Determine which poles and/or transformers are fully or partially enclosed inside the fire spread area for the given time step. Note that the fire polygon and the individual pole and transformer coordinates all conform to the GIS layout of Micropolis in ArcMap (see Chapter II).

3) Determine all Lines, Banks and/or NO switches that are affected by the faulted poles and/or transformers as found in step (2).

4) Scan all Line numbers as found in step (3) to determine which of those are downstream with respect to any other Line or a Bank or a NO switch as also found to be faulted in (3). Eliminate all such downstream Line numbers from the list of (3) as they will anyways be getting isolated by the isolation of their concerned upstream components.

5) Isolate each of the upstream Lines/Banks/NO switches as identified in step (4). For each such isolated upstream component, scan all Lines which are located downstream with respect to it. If any of such downstream Lines is found to be live till now, it will also get 'effectively isolated' as a result of the isolation of the concerned upstream component.

6) Are all upstream Lines/Banks/NO switches as found in step (4) isolated? If yes, go to step (7). If not, repeat step (5).

7) Call the graph theoretic subroutine explained in the next section with an argument containing the IDs of all Lines and NO switches which are getting physically or effectively isolated in the current time step.

8) The graph theoretic subroutine returns back an argument containing a list of the IDs of NO switches that need to be closed for routing power to the affected parts of the system, and a list of the IDs of isolators that need to be opened for preventing bi-directional power flows at the network nodes (see subsection 7.4.6). Perform all such actions (closing of switches and opening of isolators) and proceed to step (9).

9) For all Lines, Banks and/or NO switches getting physically or effectively isolated in the current time step, add up the total load (KVA) lost as a result of such outages. Calculate the current time step's contribution to the LLDI using equation (5.1).

10) Check if the MUFS simulation has been completed (entire 12 hours of simulation data has been generated) OR if both the substation breakers of Micropolis have been opened (in which case, the city has been blacked out). If either of the

conditions is satisfied, end simulation and print results. Else, increase iteration count and go to step (1).

7.4. Formulation of Graph Theoretic Approach for Power Routing

This section proposes a graph theoretic approach [24] for routing power across faulted sections of the electrical distribution network of a city using a given set of NO switches. This approach forms part of the overall algorithm presented in Section 7.3. The proposed methodology is explained through the following subsections using the example of Micropolis.

7.4.1. Drawing the Equivalent Graph

The first step in implementing the graph theoretic approach, however, would be to represent the electrical distribution network of a city such as Micropolis by an equivalent graph. In doing so, all single phase laterals which branch off from any given line in the distribution network are ignored while constructing the equivalent graph. This is because in the event that a 'parent' line (e.g. Line 11 in Fig. 7.1) from which a concerned lateral (e.g. Line 30 in Fig. 7.1) branches out gets faulted and isolated, the lateral gets effectively isolated as well. This also makes the resultant graph look less bulky. Similarly, any three-phase tapping (e.g. Line 6 in Fig. 7.1) which branches out of a line in the electrical network and which gets terminated by itself, i.e. it neither branches off into any more sub-branches nor ends in a NO switch, is ignored as well.

The equivalent graph representing the distribution network of Micropolis, as shown in Fig. 7.2, is constructed by 'stitching together' two tree structures, with each tree representing the network associated with a given feeder. Each edge of a tree thus

represents a particular Line in the electrical network of Fig. 7.1. The topmost node in a given tree is termed as a ‘source node’, and it represents the source of power for the corresponding distribution feeder. Nodes 1 and 13 in Fig. 7.2 are thus the source nodes for our case. The trees are then stitched together using ‘links’ belonging to either of the following two categories:

7.4.1.1. Link, Type I

The edges of the individual trees, which correspond to lines across which a NO switch is physically present in the electrical network, are joined using a Type I link. The Type I links are represented by the red lines of Fig. 7.2.

7.4.1.2. Link, Type II

All source nodes of the equivalent graph are connected to a single hypothetical ‘super node’ (Node 0) by means of Type II links, as represented by the magenta lines of Fig. 7.2. The purpose of incorporating the concept of the super node is explained in a later subsection.

7.4.2. Assigning Weights

The next step after the construction of the equivalent graph is to assign weights to its individual edges and links. Each edge is assigned a weight equal to the total impedance of its corresponding line in the electrical network. Referring to Chapter IV, where the different formulae used for the impedance (Ω/km) calculations of overhead conductors and underground cables were explained, the total impedance (Ω) of a given line is calculated by multiplying its impedance (Ω/km) with its corresponding length in the distribution system. For a two or a three phase line, the weight assigned to its

corresponding edge in the equivalent graph is equal to its total positive sequence impedance value.

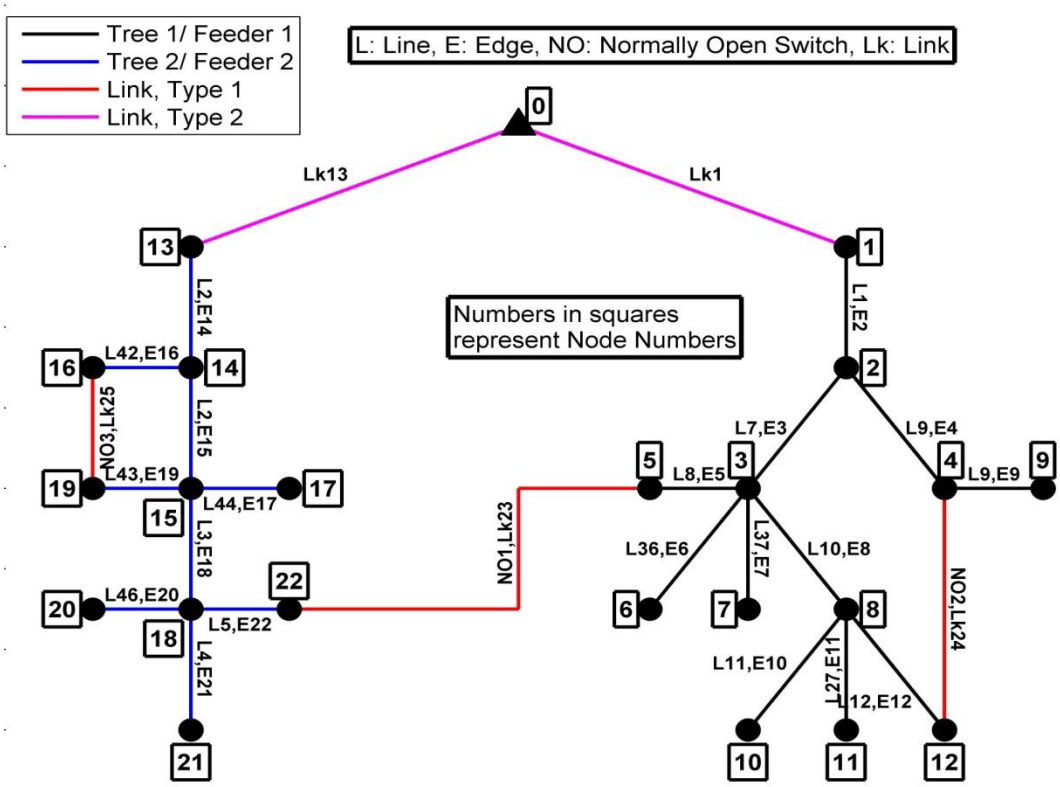

Fig. 7.2. Equivalent graph representing the electrical distribution network of Micropolis.

The Type I links are assigned weights in the following fashion. We consider the constituent trees of the equivalent graph one by one and calculate the length of the longest path in each of them. Since in a tree there is one and only one path between any pair of vertices [26], the length of the longest path can be calculated by adding up the weights of the edges as we move from the source node down to the bottommost node and by comparing the cumulative weights of the individual nodes. Denoting the maximum of the longest path lengths amongst all the constituent trees of the equivalent

graph by 'L_{max}', the weight assigned to each of the Type I links is equal to '$k*L_{max}$', where 'k' is a multiplier greater than one. This is done to ensure that in the event that we run a shortest path algorithm on the equivalent graph under normal operating conditions of the system (i.e. when all lines are healthy and all NO switches are open), the shortest path between any given edge and its corresponding source node is along its own tree structure itself and not through any Type I link. The value of 'k' is chosen to be equal to ten for the purpose of this research.

All Type II links are assigned '0' weights as they are hypothetical and as such do not physically exist in the electrical network.

The weights thereby assigned to the edges and the links of the equivalent graph of Fig. 7.2 are as shown in Table 7.1. Note that these weights are all one-time assignments made at the start of a given fire spread simulation.

7.4.3. Dijkstra's Shortest Path Algorithm (Run I)

The graph theoretic subroutine, which is used to implement the approach proposed in this section, reads the list of the faulted Line and NO switch IDs as sent by the overall electrical simulation algorithm of Section 7.3; and removes the corresponding edges and links from the equivalent graph. In the actual program, the removal of an edge or a link is simulated by replacing its previously assigned weight (as given in Table 7.1) by a very large number, say 'N' [26]. For the purpose of this research, the value of 'N' is chosen to be equal to the summation of the weights of all the edges and the links of the equivalent graph of Fig. 7.2. A preliminary run of the Dijkstra's shortest path algorithm is then performed in order to calculate the shortest path distance (Ω) between the super

node and every other node in the equivalent graph. The advantage of using the super node is that we can calculate its shortest path distance from all the other nodes in the graph by running Dijkstra's algorithm only once. Otherwise, we would have had to perform as many runs of the algorithm as there are source nodes in the graph, which in turn could be a computationally intensive process for a large distribution system.

TABLE 7.1
WEIGHTS ASSIGNED TO THE EDGES AND THE LINKS OF THE EQUIVALENT GRAPH

Type	**ID**	**Line/NO switch Number**	**Weight (Ω)**
Edge	2	Line 1	0.1182 Ω
Edge	3	Line 7	0.1212 Ω
Edge	4	Line 9	0.1323 Ω
Edge	5	Line 8	0.1212 Ω
Edge	6	Line 36	0.4386 Ω
Edge	7	Line 37	0.4386 Ω
Edge	8	Line 10	0.1323 Ω
Edge	9	Line 9	0.2389 Ω
Edge	10	Line 11	0.2901 Ω
Edge	11	Line 27	1.2847 Ω
Edge	12	Line 12	0.1323 Ω
Edge	14	Line 2	0.2593 Ω
Edge	15	Line 2	0.0606 Ω
Edge	16	Line 42	0.7092 Ω
Edge	17	Line 44	0.5293 Ω
Edge	18	Line 3	0.1474 Ω
Edge	19	Line 43	0.7692 Ω
Edge	20	Line 46	0.9161 Ω
Edge	21	Line 4	0.9101 Ω
Edge	22	Line 5	0.0737 Ω
Link, Type I	23	NO Switch 1	16.564[d] Ω
Link, Type I	24	NO Switch 2	16.564 Ω
Link, Type I	25	NO Switch 3	16.564 Ω
Link, Type II	1	Not Applicable	0
Link, Type II	13	Not Applicable	0

[d] L_{max} for the equivalent graph of Fig. 7.2 is equal to 1.6564 Ω.

The Dijkstra's algorithm is run according to the following steps [26]:

1) Assign a permanent label of '0' to the super node and temporary labels of '10^6' to all the remaining nodes in the graph.

2) Set variable 'n_i', corresponding to a given node 'i' in the graph, to 0 (ID of the super node).

3) Scan through all the temporarily labeled nodes in the graph in order to determine which of them are connected to node 'i' through an edge or a link. Any node 'j' found so connected then gets a new temporary label equal to min(old label of 'j', (old label of 'i'+d_{ij})), where 'd_{ij}' is the weight of the edge or the link connecting nodes 'i' and 'j'.

4) After all temporary labeled nodes have been scanned and new temporary labels assigned wherever applicable, the minimum of all the temporary labels is found and that becomes the permanent label for the corresponding node. In case of a tie, any one of the concerned nodes is selected and is permanently labeled.

5) Assign the ID of the node which was just permanently labeled in step (4) to the variable 'n_i'.

6) Are all nodes in the equivalent graph permanently labeled? If yes, proceed to the next subsection. If not, go to step (3).

The permanent label thereby assigned to a given node in the graph is actually the length of the shortest path joining that node to the super node. Since the calculated length is in ohms, it also represents the minimum impedance path connecting the two points.

7.4.4. Determining Network Connectivity

Assuming that at a particular time step during the course of a given fire spread simulation, Lines 10 and 12 become faulted; it can be observed from Fig. 7.1. that Lines

11 and 27 will be effectively isolated as well due to lack of connectivity with the rest of the network. This subsection explains how the graph theoretic subroutine finds out which additional lines (i.e. apart from the ones which the overall electrical simulation algorithm of Section 7.3 determines as being faulted) have lost power in the current time step due to lack of network connectivity.

After the first run of the Dijkstra's shortest path algorithm is performed, we scan through each edge of the equivalent graph which corresponds to some healthy line in the electrical network. For each such edge, we compare the lengths (Ω) of the minimum impedance path associated with its two terminating nodes, and assign the node corresponding to the shorter of those two lengths as its 'target node'. The minimum impedance path length associated with a given line in the electrical network is thus equal to the length of the minimum impedance path connecting the super node to the target node of the edge corresponding to the concerned line.

There might be some instances in the distribution system where one line may have multiple edges representing itself in the equivalent graph (e.g. Lines 2 and 9 in Fig. 7.2). For such situations if we consider the constituent edges of the line one by one and assign target nodes to each of them, the same line will end up having more than one target node. This in turn implies that there will be more than one minimum impedance path associated with the same line and hence power can flow into the line from more than one point. Since a 'Line' (as defined in Section 5.2) has isolating elements at its ends only, this kind of configuration might lead to a bi-directional flow of power to occur on the same line, which is unacceptable. In order to avoid such situations, we have

to therefore ensure that all the edges of the graph belonging to the same line are assigned just one target node. To do so, we consider as a whole the chain of edges corresponding to a given line, and compare the minimum impedance path lengths associated with the two nodes present at the extreme ends of the chain. For edges 4 and 9 belonging to Line 9 in Fig. 7.2, the two extreme end nodes would therefore be those with the IDs 2 and 9. Thereafter, the node corresponding to the shorter of the two lengths is assigned as the target node for the entire chain of edges belonging to the same line.

Denoting the length of the minimum impedance path associated with a given line 'i' as '$L_{min,i}$', we can draw the following conclusions regarding its connectivity status for the current time step.

7.4.4.1. $L_{min,i} <= L_{max}$

The satisfaction of this inequality implies that the concerned line is healthy and is receiving power as it would under normal operating conditions of the system. In other words, the minimum impedance path connecting the super node to the edge corresponding to the given line does not involve any Type I link.

7.4.4.2. $L_{max} < L_{min,i} < N$

The satisfaction of this inequality implies that the concerned line is healthy but it receives power through the closure of at least one NO switch. In other words, the minimum impedance path connecting the super node to the edge corresponding to the given line involves at least one Type I link.

7.4.4.3. $L_{min,i} >= N$

The satisfaction of this inequality implies that the concerned line has become effectively isolated due to lack of network connectivity. In other words, the edge corresponding to the given line cannot be connected to the super node without passing through at least one faulted edge or a faulted Type I link.

The graph theoretic subroutine thus calculates the $L_{min,i}$ values associated with all healthy lines in the electrical network, and groups them into the three different categories as described above. While lines satisfying the first inequality continue to receive power as they would under normal operating conditions of the system, those satisfying the second inequality are assigned shortest impedance paths using the available NO switches of the electrical network. Finally, lines satisfying the third inequality are declared as being effectively isolated from the current time step onwards.

7.4.5. Assigning Shortest Impedance Paths for Power Routing

The graph theoretic subroutine keeps a record of the order in which the various nodes of the equivalent graph get permanently labeled while performing the first run of the Dijkstra's algorithm. This record is stored in a row matrix 'A'. For a given line satisfying the second inequality of subsection 7.4.4, let us assume that the target node of its corresponding edge in the equivalent graph is stored in column 'i' of the 'A' matrix. The minimum impedance path for the concerned line can then be constructed by working backwards from the 'i^{th}' column of the 'A' matrix till we reach column '0'; such that we go to that predecessor column whose corresponding node label differs from that of the current column by an amount equal to the weight of the connecting edge or

link [26]. One may however observe that the minimum impedance paths so traced using the 'A' matrix as obtained from the primary run of the Dijkstra's algorithm may not always produce the most optimal results. This is owing to the fact that even though a closed NO switch is supposed to be represented in the equivalent graph by a Type I link of '0' weight, we had assigned artificially high weights of 'k*L_{max}' to all the Type I links for reasons explained in subsection 7.4.2. This argument can be further illustrated using the example of a sample network, as represented by the equivalent graph of Fig. 7.3.

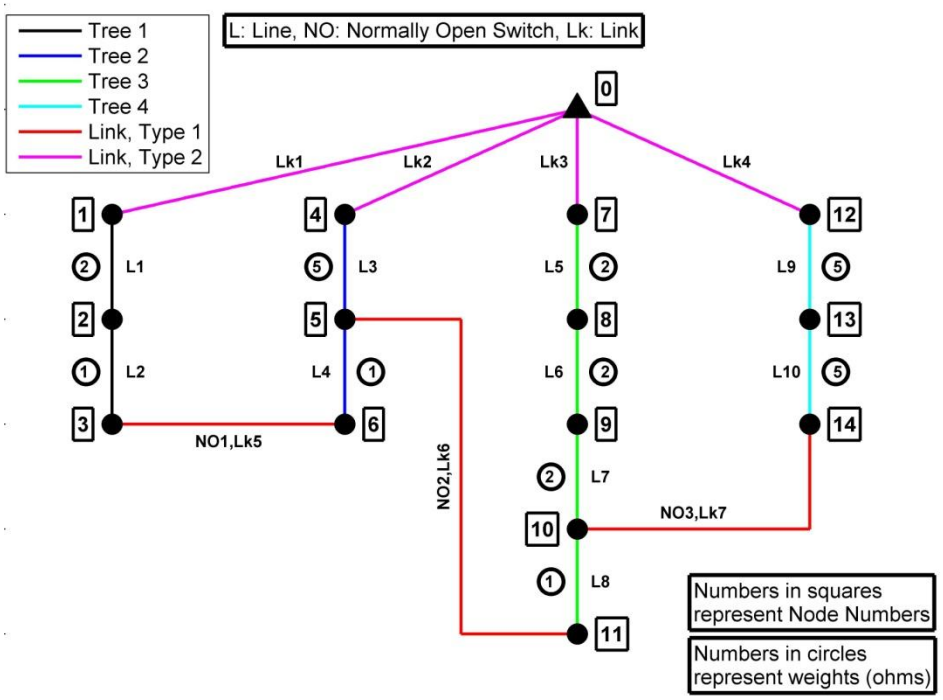

Fig. 7.3. Equivalent graph representing a part of a sample electrical network.

Assuming that at a particular time step during the course of a given fire spread simulation, Lines 3 and 6 of Fig. 7.3 become faulted; one may observe that Line 7 can be connected to the rest of the network through either of the following two paths: 'Lk1, L1

L2, Lk5, L4, Lk6, L8' or 'Lk4, L9, L10, Lk7'. Assuming that L_{max} for the network of Fig. 7.3 is equal to 10Ω, the weights assigned to each of the Type I links would therefore be equal to 100Ω (refer to subsection 7.4.2). Under this situation, the primary run of the Dijkstra's algorithm would therefore designate the latter path as the minimum impedance path for routing power to Line 7. Since a closed NO switch, as is required for the routing of power, should be represented in the equivalent graph by a Type I link of '0' weight, one may however observe under this assumption that the former path actually has a lower impedance than the latter. The minimum impedance path for routing power to Line 7, as calculated from the first run of the Dijkstra's algorithm, does not therefore give us the most optimal solution in this case.

To solve this issue, we freeze the permanent labels (as obtained from the first run of the Dijkstra's algorithm) of all nodes in the equivalent graph which are associated with edges satisfying the first inequality of subsection 7.4.4. This is done to ensure that we retain the configuration of those parts of the network which are receiving power as they would under normal operating conditions of the system. The weights of all healthy Type I links of the equivalent graph are then set to 0, and a second run of the Dijkstra's shortest path algorithm is performed. The minimum impedance paths associated with lines satisfying the second inequality of subsection 7.4.4 are then constructed using the 'A' matrix as obtained from the second run of the Dijkstra's algorithm. Note that the graph theoretic subroutine resets the weights of all healthy Type I links back to their original values before proceeding to the next subsection.

One may further observe that even the approach described above may not always generate the absolute minimum impedance paths for power routing. To illustrate this, let us now assume that only Line 6 in Fig. 7.3 is faulted. Using the above mentioned approach, the minimum impedance path as calculated for routing power to Line 7 would now be along ‘Lk2, L3, Lk 6, L8’, and not along ‘Lk1, L1 L2, Lk5, L4, Lk6, L8’. This is in spite of the fact that the latter path has a lower impedance than the former. This anomaly can be resolved by observing that our main focus is to provide uninterrupted service to customers who are already receiving power without the need of any routing. The above mentioned approach can therefore be best regarded as a compromise between finding the absolute minimum impedance path for routing power to a concerned line and retaining the configuration of those parts of the electrical network which are receiving power as they would under normal operating conditions of the system.

7.4.6. Resolving Bi-directional Power Flow Issues

Referring again to Fig. 7.2, let us assume that at a particular simulation time step, Line 7 gets faulted by fire. Let us also assume that the target nodes for edges 5 and 8, as determined from the second run of the Dijkstra’s shortest path algorithm, are nodes 5 and 8 respectively. Under such circumstances, the minimum impedance path associated with Line 8 will be along ‘Lk13, E14, E15, E18, E22, Lk23’, while that associated with Line 10 will be along ‘Lk1, E2, E4, Lk24, E12’. It can thus be easily observed that there will be a bi-directional flow of power occurring at node 3. This section presents an algorithm to check for and correct bi-directional power flows occurring at different nodes across the equivalent graph.

1) Scan through each node of the graph except for the super node.

2) For a given node, determine which all edges and Type I links are incident (in/out) at it, and store their corresponding IDs in a temporary matrix ‘X’. In doing so, ignore any faulted edge, faulted Type I link or even any healthy Type I link where the corresponding NO switch has an ‘open’ status for the current time step.

3) For a given ID stored in matrix X, does that correspond to an edge? If yes, go to step (4). If not, go to step (5).

4) Check if the target node corresponding to the edge being examined in step (3) is different from the node being examined in step (2). If yes, go to step (6). If not, store the ID of the concerned edge in another matrix ‘Y’. Also, check the constituents of the minimum impedance path associated with this current edge and store in matrix ‘Y’ the ID of the edge or link from which power flows into this edge. Proceed to step (6).

5) For the Type I link being examined in step (3), the graph theoretic subroutine retrieves the ID of the edge from which power flows into this link. Check if this concerned edge is also incident at the same node as was being examined in step (2). If yes, store the concerned edge and Type I link IDs in matrix Y and go to step (6). If not, directly go to step (6).

6) Are all the edge and link IDs as stored in matrix X in step (2) analyzed? If yes, go to step (7). If not, pick up the next available ID and go to step (3).

7) For each ID stored in matrix X, check if it appears in matrix Y as well. If it does, go to step (8). If not, open the terminating isolator of the line corresponding to the

edge whose ID was not found in Y; such that the isolator is located at that point in the electrical network which corresponds to the node being examined in step (2). Go to (8).

8) Have all IDs stored in matrix X been checked against those in matrix Y? If yes, go to step (9). If not, pick up the next available ID and repeat (7).

9) Have all nodes of the graph except for the super node been scanned for the current time step? If yes, stop running subroutine and return back control to the overall electrical simulation algorithm of Section 7.3. If not, pick up the next available node and go to step (2).

To better explain the above mentioned algorithm, let us consider a part of a sample distribution network, as represented by the graph of Fig. 7.4. Consider node 2 and assume that the edges 1, 2, 3 and 4 and the Type I link 5 are all incident at it as shown in Fig. 7.4. Also assume that for a given simulation time step, the resultant power flow in the network is as shown by the arrows in Fig. 7.4.

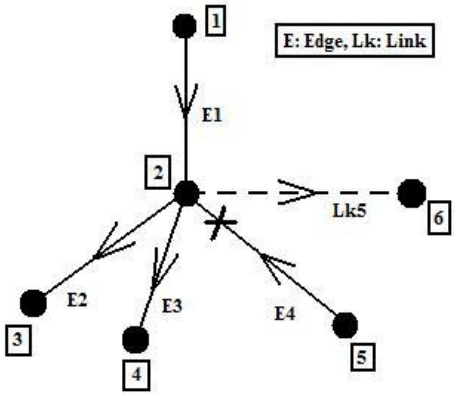

Fig. 7.4. Graph representing part of a sample distribution network.

Now, assuming that edge 2 receives its power from edge 1, one may conclude that the target node and the immediately upstream edge ID for edge 2 would be those of node 2 and edge 1 respectively. Since the graph theoretic subroutine assigns a unique minimum impedance path to a given target node, any edge which is incident at node 2 and which gets its power through that node will have the same target node and immediately upstream edge ID combination as edge 2. Thus, following the steps mentioned in the algorithm above, matrices X and Y for the network of Fig. 7.4 would look like: X = [1;2;3;4;5] and Y = [1;2;3;5]. Note that since the target node for edge 4 is node 5 (and not node 2); it does not appear in matrix Y. Thus, the bi-directional power flow encountered at node 2 can be prevented by opening the terminating isolator of the line corresponding to edge 4; such that the isolator is located at that point in the electrical network which corresponds to node 2 (as shown by the cross marked on edge 4 in Fig. 7.4).

Thus the electrical algorithm of Section 7.3 calls a graph theoretic subroutine, which in turn implements the general approach presented in Section 7.4. The important results obtained from running different fire spread simulations on the electrical distribution network of Micropolis using the algorithm of Section 7.3 are presented in the next chapter.

CHAPTER VIII

ANALYSIS OF SIMULATIONS RUN INCORPORATING POWER ROUTING

Referring to the simulation results presented in Chapter VI, we again run the 160 different simulations corresponding to the various fire spread scenarios, but using the algorithm of Section 7.3 instead of the one presented in Section 5.5. In other words, we run those simulations by incorporating the concept of power routing into the program logic. Figures 8.1(a) – (d) show the relevant results obtained from the different simulation runs [24].

As in Chapter VI, ten simulations corresponding to the different supporting infrastructure damage profiles were run for a given UFIP and wind direction combination. The LLDI value generated from each such simulation run was then compared to that calculated in Chapter VI for the same fire spread scenario. It can be observed from Figs. 8.1(a) – (d) that the LLDI values corresponding to the simulations where we have incorporated the concept of power routing are consistently lower than those obtained from the same simulations run in the absence of routing. This is because more customers can be served by routing power through the NO switches during emergencies, thereby leading to lesser load losses and lower LLDI values. An interesting exception to this pattern can be observed for damage profiles D01 and F01 (ECO, West), where the LLDI values generated with the incorporation of power routing into the simulation logic are more than those obtained in its absence.

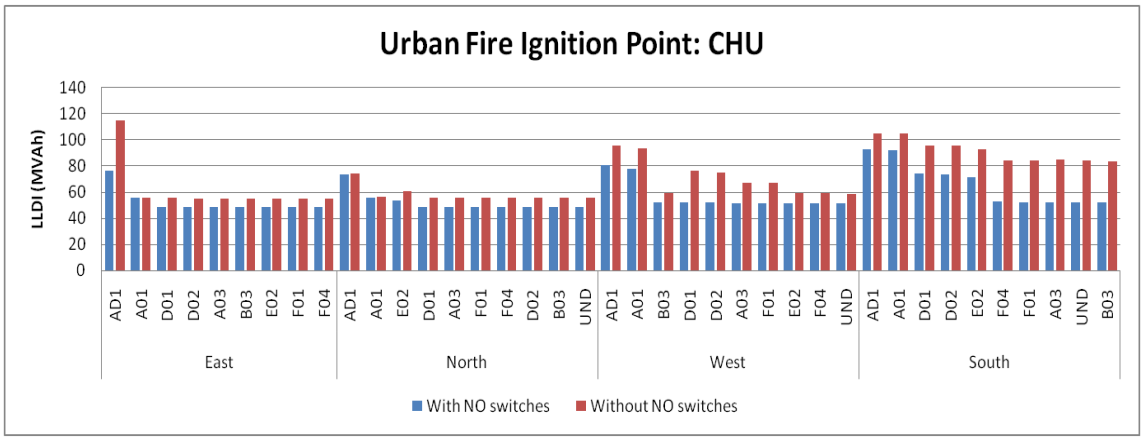

(a)

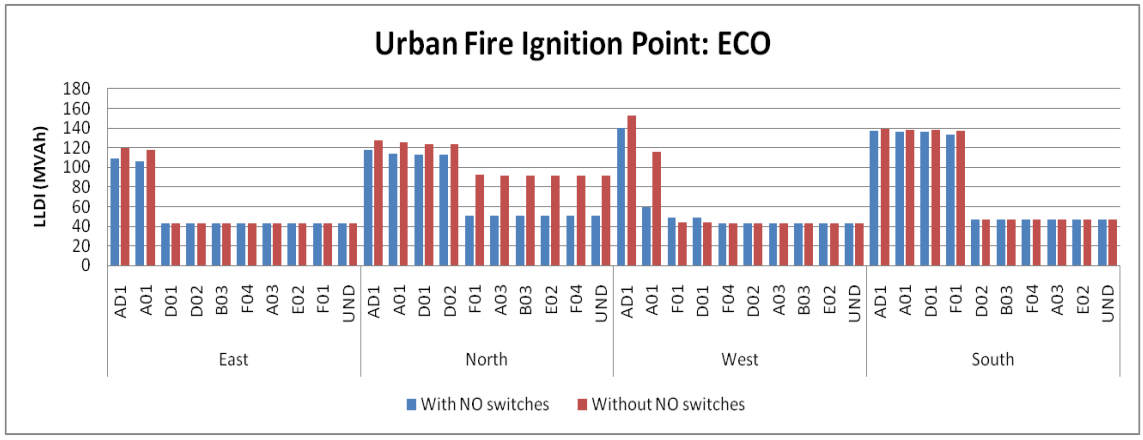

(b)

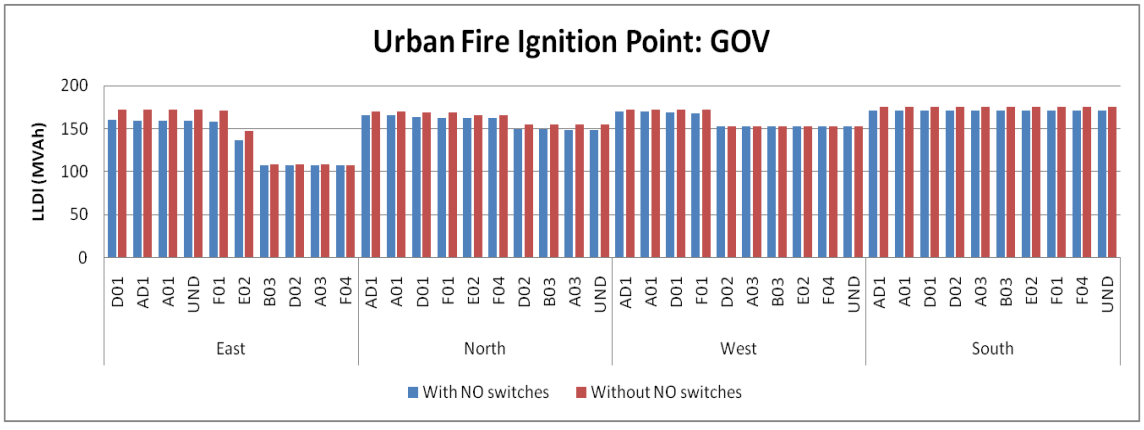

(c)

Fig. 8.1. Results of electrical simulations run incorporating power routing.

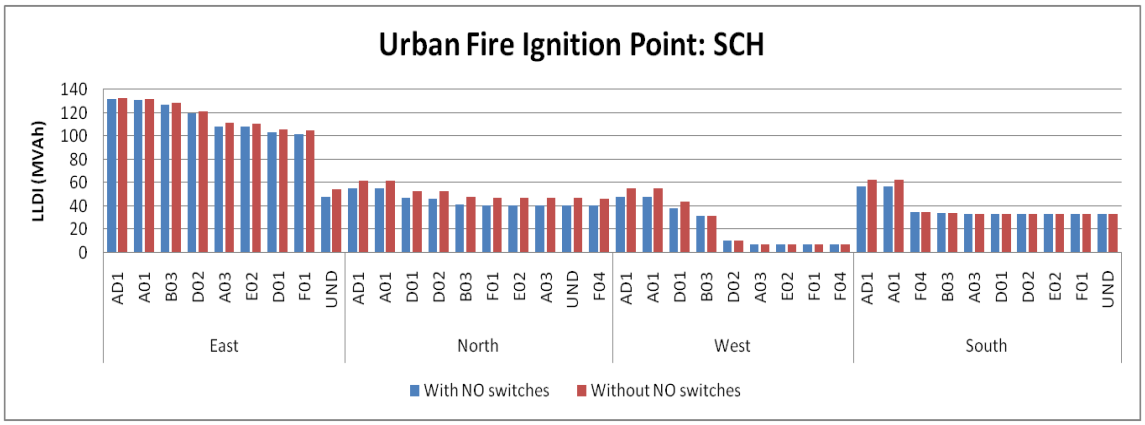

(d)

Fig. 8.1. continued.

This is because for both of those scenarios, a pole in the industrial area on which the NO switch 2 is mounted gets faulted mid-way through the simulations. Since the NO switch 2 spans across the Lines 9 and 12 (see Fig. 7.1), both the lines have to be isolated from the rest of the network in order to clear the above mentioned fault. But referring to the general methods of treatment of faulted components as presented in Section 5.3, a fault in the concerned pole in the industrial area could be cleared by isolating Line 9 only in the absence of routing (see Fig. 4.8). Thus, the customers connected to Line 12 could still be served and that resulted in a lesser loss of load and a lower LLDI value.

One more analysis of the electrical simulation results was performed by calculating the average LLDI value generated across all combinations of SIDPs and wind directions for a given UFIP profile [24]. The calculated average was then compared to that computed in Section 6.2 for the same UFIP profile, in order to show the percent reduction obtained in the LLDI value after the incorporation of power routing into the simulation logic. Table 8.1 shows the relevant results.

TABLE 8.1
AVERAGE LLDI VALUES CALCULATED FOR DIFFERENT UFIP PROFILES

Ignition Point Acronym	Average LLDI values (MVAh)		Percent Reduction
	Without routing	With routing	
GOV	160.811	156.131	2.9%
ECO	76.845	67.453	12.22%
CHU	70.889	57.277	19.2%
SCH	55.909	52.827	5.51%

One may observe from Table 8.1 that the percent reductions obtained for the UFIP profiles comprising of the city's government buildings and the schools are much lesser than those obtained for the 'ECO' and 'CHU' profiles. Looking at Fig. 2.1, where the government buildings have been represented by a 'G' marked on them, one may note their proximity to the city's central business district, the industrial area and the two feeders coming out of the city's substation. A fire starting from these buildings thus causes a heavy loss of load towards the early stages of the simulations, so much so that the entire city is blacked out in a few hours of fire spread. The NO switches are thus rendered useless for the maximum part of the simulations, thereby not producing a significant reduction in the calculated average LLDI value.

For the city schools, which are buildings with a 'S' marked on them in Fig. 2.1, one may see that they are mostly located in a sparsely populated residential area towards the leftmost boundary of the city. A fire starting from these buildings thus takes a lot of time to cover enough ground so as to fault some important feeder line and require the closure of NO switches for routing of power. The percent reduction obtained in the average LLDI value calculated for this profile is therefore not anything significant either.

The city's ecological targets and its churches, on the other hand, can be found to be much more evenly distributed across the city (see Fig. 2.1). Thus, even if the fire takes down some important feeder line, its adverse effect can be offset by routing power using the healthy NO switches of the network; thereby producing higher percent reductions in the calculated average LLDI values.

CHAPTER IX

CONCLUSIONS

The research work presented in this thesis aims at studying the effects of fire on the electrical distribution network of a city. Starting with the modeling of the city's electrical infrastructure components, this thesis explains how one can use the outputs of the MUFS code for analyzing and quantifying the damage caused by fire to the electrical network. The proposed methodology is explained using the example of a virtual city named Micropolis.

The thesis also proposes an efficient algorithm which incorporates graph theoretic concepts for routing power across faulted sections of the electrical network using a given set of Normally Open switches. The power is so routed that it flows along a path of minimum impedance. The proposed algorithm is again implemented using the example of Micropolis.

A set of two simulations are run on the distribution system of Micropolis corresponding to a given fire spread scenario – one incorporating the concept of power routing using the Normally Open switches of the electrical network and the other assuming the absence of routing. The LLDI values obtained from each such set are then compared to each other in order to understand the advantages of power routing during emergencies. The LLDI values generated from simulations run across all combinations of SIDPs, UFIP profiles and wind directions are also compared to each other in order to

determine which targets and infrastructure components of the city are of paramount importance in containing the damage caused by fire to the electrical network.

One of the important contributions of this research work is the use of LLDI as a means of quantifying the damage caused by fire to the electrical network. The electrical test bed described in Chapter IV can prove to be a useful resource for researchers who wish to perform similar studies on the effects of disasters on the interdependent infrastructure components of a city. Finally, the results obtained from the different simulation runs, as presented in Chapters VI and VIII, can give really useful insights to civic authorities and emergency response personnel when they deal with an actual disaster.

Though the various methodologies and algorithms proposed throughout this thesis have been explained using the example of Micropolis, they are as such very general in scope, and with some minor modifications can be easily applied to bigger distribution systems and to different disaster scenarios.

One of the major limitations of this research work is the fact that we have not carried out any electrical analysis (e.g. short circuit studies, power flows etc.) of the system while running the fire spread simulations. Though this would not have had any significant impact on the results owing to the small size of Micropolis and the assumption that the city's distribution network is connected to an infinite bus, the designing of a bigger city with transmission and distribution systems and inter-city tie lines in place would prove to be an excellent test bed to carry out a more detailed analysis on.

Referring to the graph theoretic approach proposed in Chapter VII, one may note that we are ignoring the ampacity ratings of the different conductors while assigning the minimum impedance paths for routing power during emergencies. Since these restorations are being performed under emergency conditions, this seems to be a quite reasonable approach. However, one may construct an interesting optimization problem with the objective function being that representing the power losses occurring in the different conductors and the constraint equation representing the inequality that the conductor currents should not exceed their corresponding ampacity ratings.

Finally, one may observe that while carrying out the simulations on the electrical network, the flow of information occurs from the MUFS code to the electrical program only. Since many of the civil and communication infrastructure components of a city(e.g. water pumps, cell towers etc.) depend on electric power supply for their smooth operation, the occurrence of a fault in an electrical line supplying power to any of such components would have an adverse effect on the overall fire spread scenario. The construction of a closed loop system comprising of the civil, electrical and communication infrastructure components, where each interacts with the other and with the MUFS code, would thus also be an excellent topic for future research.

REFERENCES

[1] Electronic Privacy Information Center. "U.S.A. PATRIOT Act (2001) document". [Online]. http://www.epic.org/privacy/terrorism/hr3162.html, 2001.

[2] Federation of American Students. "Presidential Decision Directive/NSC-63 on Critical Infrastructure Protection". [Online]. http://www.fas.org/irp/offdocs/pdd/pdd-63.htm, 1998.

[3] H. J. Min, W. Beyeler, T. Brown, Y. J Son, and A. T. Jones, "Toward modeling and simulation of critical national infrastructure interdependencies," *IIE Transactions*, vol. 39, pp. 57-71, Jan. 2007.

[4] L. Duenas-Osorio, J. I. Craig, B. J. Goodno and A. Bostrom, "Interdependent response of networked systems," *Journal of Infrastructure Systems*, vol. 13, no. 3, pp. 185-194, Sept. 2007.

[5] S. H. Conrad and G. P. O'Reilly, "An overview of energy and telecommunications interdependencies modeling at NISAC," in *NATO Critical Infrastructure Workshop Proceedings*, May 2006, pp. 1-8.

[6] P. Pederson, D. Dudenhoeffer, S. Hartley, and M. Permann, "Critical infrastructure interdependency modeling: A survey of U.S. and international research ," Idaho National Laboratory, Idaho Falls, ID, report prepared for the Technical Support Working Group under Work for Others Agreement 05734, Aug. 2006.

[7] K. Brumbelow, J. Torres, S. Guikema, E. Bristow, and L. Kanta, "Virtual cities for water distribution and infrastructure system research," in *Proceedings of the 2007 World Environmental and Water Resources Congress*, May 2007, pp. 1-7.

[8] A. Bagchi, A. Sprintson and C. Singh, "Modeling the impact of fire spread on the electrical distribution network of a virtual city," in *Proceedings of the North American Power Symposium*, Oct. 2009, paper 2017, accepted.

[9] K. Jones and I. Horbaczewski, "Micropolis: A power distribution system for a virtual city for research applications," unpublished undergraduate research report, Department of Electrical and Computer Engineering, Texas A&M University, College Station, TX, 2008.

[10] E. C. Bristow, "Interdependent infrastructures and multi-mode attacks and failures: Improving the security of urban water systems and fire response," Ph.D. dissertation, Texas A&M University, College Station, TX, Dec. 2006.

[11] A. S. Langsdorf, *Theory of Alternating-Current Machinery*, 2nd ed., New York: McGraw-Hill, 1955.

[12] ARCAD. "Transformer X/R ratios specification sheet". Available: http://www.arcadvisor.com/pdf/GET3550Fapp41-43.pdf . Accessed: Aug. 2009.

[13] T. A. Short, *Electric Power Distribution Handbook*, Boca Raton, FL: CRC Press, 2004.

[14] H. W. Beaty, *Handbook of Electric Power Calculations*, 3rd ed., New York: McGraw-Hill, 2001.

[15] W. H. Kersting, *Distribution System Modeling and Analysis*, 2nd ed., Boca Raton, FL: CRC Press, 2007.

[16] W. H. Kersting and W. H. Phillips, "Distribution feeder line models," *IEEE Trans. on Industry Applications*, vol. 31, no. 4, pp. 715-720, Jul. 1995.

[17] Y. Zhang, J. L. Bastos, N. N. Schulz and D. Patel, "Modeling and testing of protection devices for SPS using MATLAB/Simulink and VTB," in *Proc. Electric Ship Technologies Symposium*, 2007, pp. 103-108.

[18] S. S. Martin and M. B. Fernandez, "Model and performance simulation for overcurrent relay and fault-circuit-breaker using Simulink," *International Journal of Electrical Engineering Education*, vol. 43, no. 1, pp. 80-91, Jan. 2006.

[19] General Cable. "AAC bare overhead conductor specification sheet". Available: http://www.generalcable.com/NR/rdonlyres/00CCF8A8-5CF2-4719-A396-33C69E63F327/0/p054_056_BareOvhead.pdf. Accessed: Jul. 2008.

[20] General Cable. "Underground distribution cable 5-46 KV specification sheet". Available: http://www.generalcable.com/NR/rdonlyres/2EE1B961-8934-474E-BFB1-10516EC79C53/0/p026_030_ConNutUG.pdf. Accessed: May 2008.

[21] J. D. Glover, M. S. Sarma and T. J. Overbye, *Power System Analysis and Design*, 4th ed., Toronto, Canada: Thomson Learning, 2008.

[22] A. Chakrabarty, M. L. Soni, P. V. Gupta and U. S. Bhatnagar, *A Text Book on Power System Engineering*, New Delhi, India: Dhanpat Rai and Co. (P) Ltd., 2003.

[23] *IEEE Guide for Electric Power Distribution Reliability Indices*, IEEE Std. 1366-2003, May 2004.

[24] A. Bagchi, A. Sprintson and C. Singh, "Studying the impact of fire on an electrical distribution network using graph theory based routing algorithms," unpublished manuscript, Department of Electrical and Computer Engineering, Texas A&M University, College Station, TX, 2009.

[25] Wikipedia. "Triple Pole Single Throw (3PST) switch document". [Online]. http://en.wikipedia.org/wiki/Switch, 2009.

[26] N. Deo, *Graph Theory with Applications to Engineering and Computer Science*, Englewood Cliffs, NJ: Prentice-Hall, Inc., 1974.

VITA

Name:	Arijit Bagchi
Address:	Quarter 5/7, Central Park, City Center
	Durgapur, West Bengal, India
	Zip: 713216
Email Address:	bagchi.arijit@gmail.com
Education:	B.E., Electrical and Electronics Engineering, Birla Institute of Technology, MESRA, Ranchi, India, May 2005
	M.S., Electrical Engineering, Texas A&M University, Dec. 2009